

Review

# Thermal and Photochemical Reactions of Organosilicon Compounds

Masae Takahashi 

Department of Physics, Graduate School of Science, Tohoku University, Sendai 980-8578, Japan;  
masae.takahashi.d1@tohoku.ac.jp

**Abstract:** This article provides a comprehensive review of quantum chemical computational studies on the thermal and photochemical reactions of organosilicon compounds, based on fundamental concepts such as initial complex formation, HOMO-LUMO interactions, and subjacent orbital interactions. Despite silicon's position in group 14 of the periodic table, alongside carbon, its reactivity patterns exhibit significant deviations from those of carbon. This review delves into the reactivity behaviors of organosilicon compounds, particularly focusing on the highly coordinated nature of silicon. It is poised to serve as a valuable resource for chemists, offering insights into cutting-edge research and fostering further innovations in synthetic chemistry and also theoretical chemistry.

**Keywords:** computational chemistry; reaction process; organosilicon compound

## 1. Introduction

Ab initio molecular orbital (MO) calculations are a powerful tool for investigating reaction pathways from reactants to products, offering insights for controlling these pathways to obtain desired molecules. This review introduces the theoretical process of identifying reaction pathways based on chemical intuition, prior to the advent of automated programs designed to determine reaction pathways. This approach is fascinating and even informative from a chemical perspective.

Silicon, a group 14 element, shares chemical properties with carbon. However, while these similarities hold true in some respects, they do not extend to the structure and reactivity. This review covers thermal and photochemical reactions of organosilicon compounds. In the thermal reaction section, bimolecular 1,2-addition reactions to double bonds and unimolecular 1,3-rearrangements are discussed. The photochemical reaction section addresses interconversion and unimolecular sigmatropic rearrangements. The treatment of excited states, which differ significantly from ground state phenomena, includes a detailed explanation of the key process of selecting the complete active space.

## 2. Thermal Reactions

### 2.1. 1,2-Additions to the Double Bonds

The differences in stable structures between unsaturated silicon and carbon compounds result in varied reactivity and selectivity of chemical reactions. Unsaturated carbon compounds, such as ethylene, acetylene, allene, benzene, and the two-dimensional material graphene, are stable, exhibiting planar or linear structures. Conversely, their silicon counterparts, including disilene, disilyne, trisilaallene, hexasilabenzene, and silicene, are unstable, likely due to their nonplanar or nonlinear structures. Silicene, the silicon equivalent of graphene, has been experimentally synthesized in a vacuum as a promising material and



Academic Editor: Yongzhong Bian

Received: 10 February 2025

Revised: 2 March 2025

Accepted: 3 March 2025

Published: 4 March 2025

**Citation:** Takahashi, M. Thermal and Photochemical Reactions of Organosilicon Compounds. *Molecules* **2025**, *30*, 1158. <https://doi.org/10.3390/molecules30051158>

**Copyright:** © 2025 by the author. Licensee MDPI, Basel, Switzerland. This article is an open access article distributed under the terms and conditions of the Creative Commons Attribution (CC BY) license (<https://creativecommons.org/licenses/by/4.0/>).

theoretically studied [1–13]. However, a significant issue is that silicene sheets oxidize and decompose in air due to their buckled structure [14]. The instability of unsaturated silicon compounds has necessitated considerable experimental efforts for their isolation. Disilene, disilyne, and trisilaallene were ultimately isolated using bulky substituents [15–18]. The experimentally isolated structures of these compounds adopt nonplanar or nonlinear configurations. A notable feature of the molecular structures of four-membered cyclic silenes in the solid state, as determined by single-crystal X-ray diffraction, is the prominent pyramidal silicon atom [19]. Sterically protected Si=P double bonds have been generated and structurally characterized [20–24]. Additionally, compounds such as phosphaaallenes [25–34], silaallenes [35–38], germasilaallenes [39,40], and 1-phospha-3-silaallene [41] have been synthesized and studied theoretically [42–49]. Theoretical studies have highlighted that traditional density functionals like B3LYP or BP86 are inadequate for properly describing these bulky molecular structures [50]. Unfortunately, the air-stable planar hexasilabenzene and silicene have not yet been achieved experimentally. While steric stabilization using bulky substituents is common in experiments, several planar or linear unsaturated silicon compounds, expected to be air-stable, have been theoretically proposed through electronic stabilization [51–59].

In the 1,2-addition of the molecule XY to the doubly bonded compound  $>M1=M2<$ , the two reactant molecules follow two pathways 1 and 2, resulting in two regioselective products (Figure 1). Disilene, a silicon–silicon double-bonded compound, reacts readily with water, alcohol, and haloalkane to form the corresponding adducts [60–69]. This type of reaction does not occur easily with olefin, a carbon–carbon double-bonded compound, making the reaction mechanism of 1,2-additions to disilene a topic of significant interest for organic chemists.

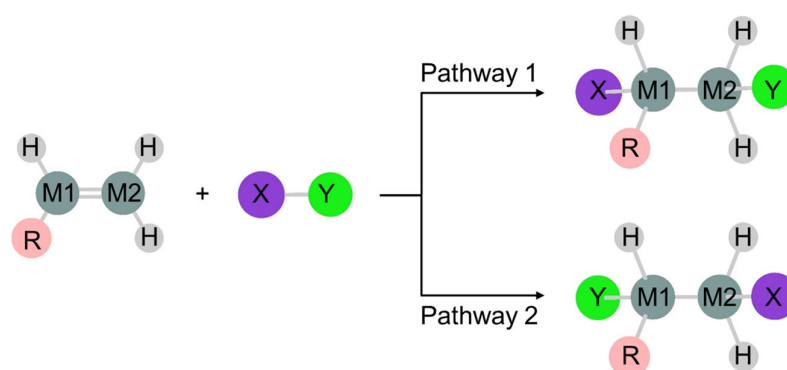


**Figure 1.** 1,2-Addition reaction of molecule XY to doubly bonded compound  $RHM1=M2H2$ , resulting in two regioselective products  $RHXM1-M2YH2$  and  $RHYM1-M2XH2$  via pathways 1 and 2, respectively. For water addition to disilene, X, Y, M1, and M2 are H, OH, Si, and Si, respectively.

### 2.1.1. The Formation of Initial Complexes

In theoretical studies of reaction pathways, the transition state of the reaction is of primary interest, as it is key to determining the product. However, the initial stage, where the two molecules encounter and the reaction begins, has received less attention. Discovering an initial complex, where the two reactants are weakly bonded, is crucial for comprehensively exploring the reaction pathway, including those not evident through common sense. In some reactions of silenes, silicon–carbon double-bonded compounds, the formation of initial complexes has been experimentally suggested. Wiberg proposed a two-step mechanism, involving the formation of an initial silene–alcohol complex, followed by proton migration from the alcohol to the carbon of the silene [70,71]. A kinetic study of the addition of acetone to silatriene indicated a stepwise pathway involving an initial attack by the carbonyl oxygen on the silenic silicon atom [72]. Kinetic studies of the

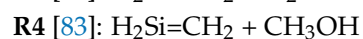
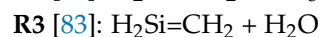
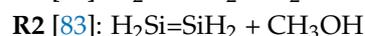
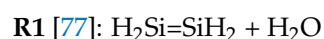
ene-addition of acetone to diphenylsilene support a stepwise mechanism involving the rapid and reversible formation of a zwitterionic silene–ketone complex, followed by a rate-limiting proton transfer from the ketone to the silene [73,74]. Based on substituent, isotope, and temperature effects on the rate constants for addition reactions to 1,1-diphenylsilene, it is concluded that these reactions proceed via the following stepwise mechanism: the nucleophilic site of the reagent first attacks silicon reversibly to generate an intermediate, which then proceeds to the product in a subsequent electrophile transfer step [73,75,76]. Takahashi et al. theoretically revealed the existence of an initial complex at the start of the 1,2-addition reaction of water to disilene, where two reactant molecules are in weak contact through van der Waals (VDW) interactions [77].

Disilenes react very smoothly with water and various alcohols without a catalyst, forming the corresponding adducts [60–69]. However, the origin of the diverse stereochemical outcomes has been controversial. The reaction of the stereoisomeric disilene, (*E*)-1,2-di-*tert*-butyl-1,2-dimesityldisilene, with various alcohols resulted in a mixture of two diastereomers [78]. The diastereoselectivity of the reaction of transient disilenes (*E*)- and (*Z*)-PhMeSi=SiMePh with alcohols was controlled by the alcohol concentration [79], suggesting intra- and intermolecular migrations of the alcoholic hydrogen atom. The addition of *p*-methoxyphenol to (*E*)-1,2-di-*tert*-butyl-1,2-dimesityldisilene was shown to be *syn*-selective in benzene but *anti*-selective in polar THF, even at low alcohol concentrations [80], indicating a bimolecular reaction of disilene with alcohols to an *anti*-adduct. The stereochemical diversity has been explained by the competition between the rotation around the Si–Si bond of the zwitterionic intermediate and the intramolecular proton transfer, but no clear explanation has been given for significant solvent effects. Takahashi et al. used ab initio MO calculations to reveal the formation of two VDW complexes at the initial stage of the reaction of disilene with water, elucidating the origin of the remarkable stereochemical diversity [77].

Predicting the reaction pathways is an intriguing topic for theoretical chemists. Frontier molecular orbital (FMO) theory is well known for predicting the qualitative characteristics of many organic reactions, including their reactivity, substituent effects, and stereoselectivity [81,82]. Since this theory considers the HOMO and LUMO of the reacting molecules, it is only applicable to the initial stages of the reaction and is less useful for multistep reactions. Modern theoretical approaches to reaction mechanisms involve searching for transition states through ab initio MO calculations and then finding paths from the transition states along the intrinsic reaction coordinates.

FMO theory is effective for the initial stage of chemical reactions [77,81,82]. In the 1,2-addition of molecule XY to doubly bonded compound RHM1=M2H<sub>2</sub>, two sets of initial interactions are predicted: nucleophilic attack by the lowest unoccupied molecular orbital (LUMO) of XY on the highest occupied molecular orbital (HOMO) of RHM1=M2H<sub>2</sub>, and electrophilic attack by the HOMO of XY on the LUMO of RHM1=M2H<sub>2</sub> (Figure 2). Both interactions generate weakly coupled initial complexes, the nucleophilic initial complex C<sub>N</sub> and the electrophilic complex C<sub>E</sub>. The existence of these complexes depends on the relative energy levels of the interacting orbitals.

Reactions **R1–R4** begin with the formation of two types of initial complexes, C<sub>N</sub> and C<sub>E</sub>. Water and methanol act as both nucleophiles and electrophiles [77,83].



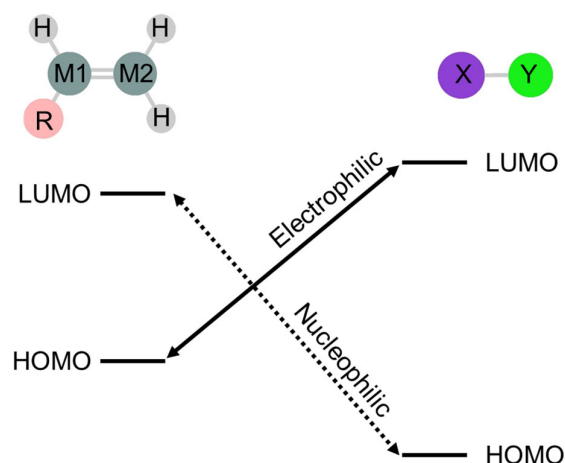
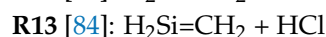
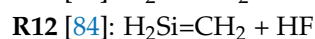
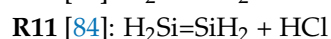
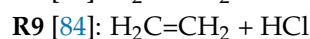
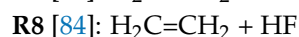
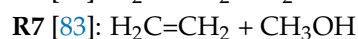


**Figure 2.** HOMO–LUMO interaction between molecule XY and doubly bonded compound  $RHM_1=M_2H_2$ .

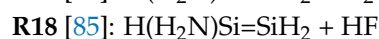
One key finding in **R1** is the bimolecular *anti*-addition pathway from  $C_N$  [77]. The existence of the *anti*-addition pathway has also been suggested experimentally [80]. Theoretical findings [77] and experimental results [80] suggest a different mechanism than previously believed. The existence of the two initial complexes  $C_N$  and  $C_E$  and the characteristic reaction channel in **R2** are similar to those in **R1** [83]. The Si=C bond in the reactants of reactions **R3** and **R4** is strongly polarized, due to the large difference in electronegativity between carbon and silicon, making the silicon in this bond more positive than that in disilene [83]. Thus, only the  $C_E$  complex is expected for the attack on carbon, and only the  $C_N$  complex is expected for the attack on silicon.

In reactions **R5–R13**, the  $C_N$  type of initial complexes is missing [83,84].



The OH group of trifluoromethanol is less electronegative than that of water and methanol, so reaction **R5** provides only  $C_E$ -type complexes [83]. Because carbon is more electronegative than silicon, only electrophilic complexes  $C_E$  are formed in reactions **R6** and **R7** [83]. In reactions **R8–R13**, the nucleophilic complexes  $C_N$  are not obtained due to the strong acidity of the hydrogen in HY (Y = F, Cl) [84].

The initial complexes involved in the 1,2-addition to monosubstituted disilenes (**R14–R18**) are doubled due to the asymmetry of the monosubstituted disilenes [85], giving rise to two possible directions: the 1-addition pathway, producing the 1-hydroxyadducts, and the 2-addition pathway, producing the 2-hydroxyadducts.



The effect of each substituent is weakly inductive (Me), strongly inductive (F),  $\pi$ -conjugated (C $\equiv$ CH), and both inductive and  $\pi$ -conjugated (NH<sub>2</sub>). Four initial complexes, two C<sub>N</sub> and two C<sub>E</sub>, are found in **R14** and **R16**, while only two complexes each are found in **R15**, **R17**, and **R18**, with two C<sub>N</sub> in **R15**, one C<sub>N</sub> and one C<sub>E</sub> in **R17**, and two C<sub>E</sub> in **R18**. The paired interacting orbitals clearly indicate whether the initial interaction is electrophilic or nucleophilic [86].

Following the theoretical capture of stable initial complexes at the initial stage of bimolecular reactions, regardless of the polarity of the double bond, by Takahashi et al. [77], the formation of initial or precursor complexes was theoretically reported in various bimolecular reactions involving double-bonded compounds [87–98]. Noncovalent interactions of heavy alkenes with H<sub>2</sub>O and HCl were investigated in detail and reported [99]. A mechanism involving initial complexation is consistent with several experimental results, such as a systematic study of the kinetics and mechanisms for five different silenes (ArAr'Si=CH<sub>2</sub>; Ar = Ar' = 2-MeC<sub>6</sub>H<sub>4</sub>; Ar = Ph, Ar' = 2,6-Me<sub>2</sub>C<sub>6</sub>H<sub>3</sub>; Ar = Ph, Ar' = 2,4,6-Me<sub>3</sub>C<sub>6</sub>H<sub>2</sub>; Ar = 2-MeC<sub>6</sub>H<sub>4</sub>, Ar' = 2,6-Me<sub>2</sub>C<sub>6</sub>H<sub>3</sub>; Ar = Ar' = 2,6-Me<sub>2</sub>C<sub>6</sub>H<sub>3</sub>) by laser flash photolysis techniques [100], Arrhenius parameters for the reaction of transient silene 1,1-diphenyl-2-neopentylsilene investigated by laser flash photolysis [101], and various distinctive reactions of trisilaallene and 2-germadisilaallene with a variety of reagents, including water, alcohols, acetone, and haloalkanes [102].

Noncovalent VDW forces are very weak and easily disturbed by thermal energy at room temperature. While experimentally detecting stable initial complexes at room temperature is challenging, the efficiency of VDW interactions can be determined spectroscopically. The effect of curvature strain and VDW forces on the interlayer vibrational modes of WS<sub>2</sub> nanotubes has been reported as a redshift of 2.5 cm<sup>-1</sup> using confocal micro-Raman spectroscopy [103]. Vibration modes are promising probes for assessing VDW interactions and can be used in various materials, including biological systems. Terahertz vibrations, in particular, are powerful for detecting weak interactions [104–106]. Named after van der Waals, who introduced attractive interactions between neutral molecules in his equation of state, VDW interaction is a dispersion interaction of pure quantum physical origin [107–111]. Combined with reliable and well-established density functional theory (DFT) calculations for analyzing vibrational absorption spectra, the effect of dispersive interactions has been directly revealed by observing changes in vibrational spectra at low temperatures where thermal disturbances are suppressed, and VDW interactions become effective against thermal motion [112,113].

### 2.1.2. Transition States

Combining ab initio MO calculations and the FMO theory to search for the transition state offers a good perspective on the mechanism of the reaction of disilene with water, denoted as **R1** in Section 2.1.1 [77,114]. Given that the interaction between disilene and water in the initial complex is very weak, with a stabilization energy of less than 1 kcal/mol, and that the geometry of each reactant is almost unchanged, the energy levels and orbital shapes of the initial complexes are those of the reactants. According to the FMO theory, the orbital interactions between the HOMO and LUMO are crucial. Utilizing the OVGf (outer valence Green's function) method [115–118] with a 6-311++G\*\* basis set for the MP2(full)/6-311++G\*\* geometry, the HOMO and LUMO of *trans*-bent disilene are  $\pi$ - and  $\pi^*$ -type orbitals, respectively, while the HOMO and LUMO of water are the oxygen lone pair (n) and O-H  $\sigma^*$  orbitals, respectively. The formation of the nucleophilic initial complex (C<sub>N</sub>) raises the LUMO ( $\pi^*$ ) level of disilene and lowers the HOMO (n) level of water. Consequently, the LUMO of C<sub>N</sub> becomes mainly the LUMO of water ( $\sigma^*$ ), and the HOMO becomes primarily the HOMO of disilene ( $\pi$ ). The secondary step of the reaction after

the formation of  $C_N$  is HOMO ( $\pi$ )–LUMO ( $\sigma^*$ ) interaction, an electrophilic attack by the water part of  $C_N$ . The hydrogen of water attacks the silicon  $p_\pi$  lobe on the other side of the  $\pi$  plane (antarafacial approach), involving rotation around the Si–Si bond, leading to a Lewis adduct ( $C_L$ ) via the transition state  $TS_E$  (Figure 3). From  $C_L$ , the *anti*-adduct (*anti*-silanol)  $P_A$  is obtained via the four-membered cyclic transition state ( $TS_L$ ) discovered by Nagase et al. [119]. On the other hand, the formation of the electrophilic initial complex ( $C_E$ ) lowers the HOMO ( $\pi$ ) level of disilene and raises the LUMO ( $\sigma^*$ ) level of water. Thus, the secondary step from  $C_E$  is the nucleophilic attack of water on disilene through the interaction of the HOMO of water ( $n$ ) with the LUMO of disilene ( $\pi^*$ ). Since the  $n$  orbital of oxygen is nearly orthogonal to the  $p_\pi$  orbital on approach to the Si atom, the sterically favored *syn*-approach is selected, forming the Lewis adduct ( $C'_L$ ) via transition state  $TS_N$  and the *syn*-adduct (*syn*-silanol)  $P_S$  via transition state  $TS'_L$  (Figure 3).

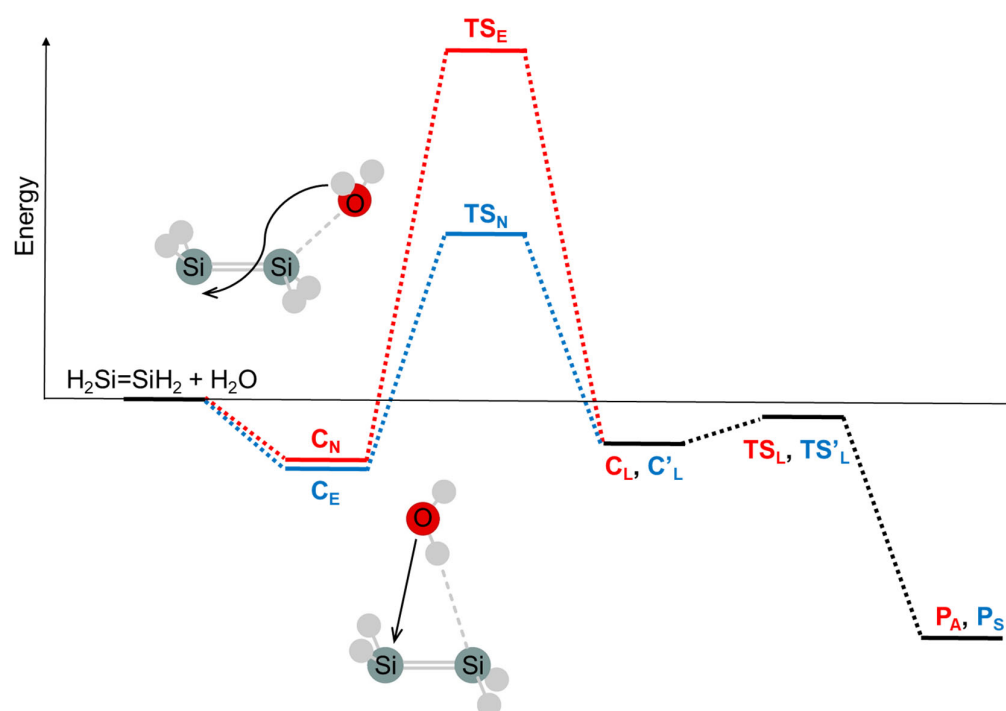


**Figure 3.** Energy diagram for the water-addition reaction to disilene.  $C_L$ ,  $TS_L$ , and  $P_A$  are the same as  $C'_L$ ,  $TS'_L$ , and  $P_S$ , respectively, in the water-addition reaction to disilene, as the two silicon atoms in disilene are not distinguished.

For large systems, DFT calculations provide a relatively inexpensive alternative to more established quantum-chemical approaches for FMOs. Within the DFT framework, long-range corrected functionals typically yield accurate HOMO and LUMO energies corresponding to ionization potentials and electron affinities, whereas conventional and widely used functionals such as hybrid B3LYP [120] significantly underestimate these orbital energies [121]. FMOs have achieved great success in describing chemical reactivity, particularly for small systems. However, for large systems, the delocalization of canonical molecular orbitals makes it difficult for FMOs to highlight the locality of the chemical reactivity. To obtain localized molecular orbitals that also reflect the frontier nature of chemical processes, the concepts of frontier molecular orbitalets [122] and principal interacting orbital analysis [123] have been recently developed for designing the reactivity of large systems. Additionally, to seamlessly integrate the quantum chemical calculations with chemical intuition, Glendening et al. proposed a practical algorithm for calculating natural bond orbital (NBO)-based resonance natural bond orbitals, which can accurately describe the localized bond shifts in reactive chemical processes [124].

A generalized mechanism for nucleophilic addition to disilene was recently proposed by McOnie et al. [93] based on computations of the ammonia-addition reaction to tetramethylsilyldisilene. There are two unique approaches for nucleophiles to disilene: approaching from the base of pyramidal Si (Route 1) or approaching from the apex of pyramidal Si (Route 2) (Figure 4). If the nucleophile or the substituents on disilene are small, Route 1 may be followed. This route requires an inversion at Si, followed by an intramolecular transfer of the hydrogen, to provide a *syn*-product, either in two steps or as a concerted reaction. When the substituents are bulky, Route 2 is preferred.

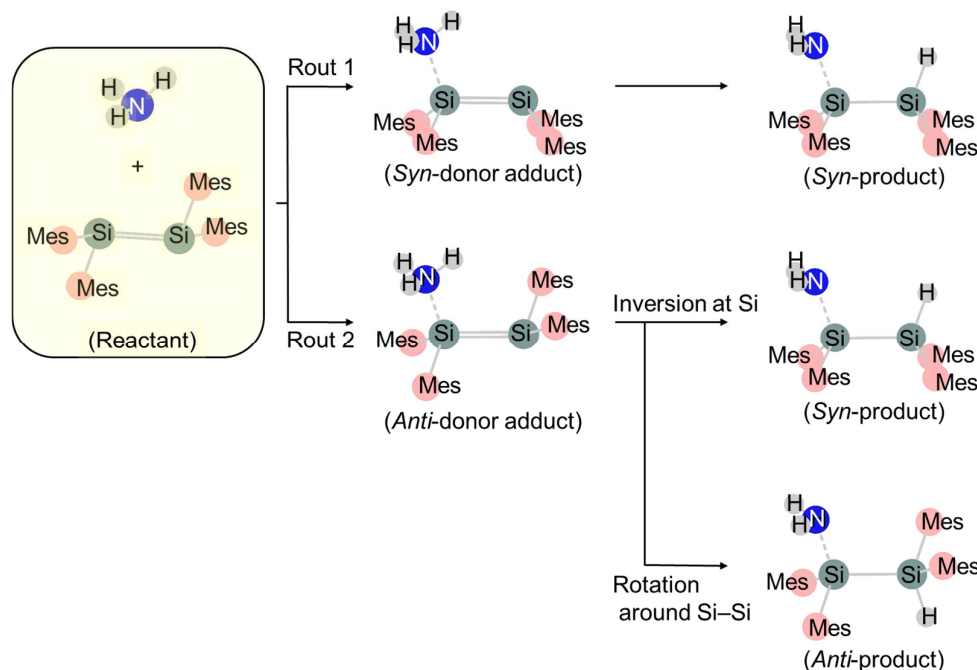


**Figure 4.** Generalized mechanism for nucleophilic addition of ammonia to disilene.

The mechanism of the disilene–water model reaction [77,114], i.e., the formation of an initial complex followed by transition states and intermediate complexes to stereoselectively afford products, has been applied to a variety of bimolecular reactions, such as 1,2-addition to dimetallenes, silene, and trimethylsilylketene [80,83–87,90–92,97,125–127], abstraction reactions of disilenes and digermenes with haloalkanes [88,89], NH bond activation of ammonia and amines by ditetrelene [93], addition to ring-containing silenes, silabenzene, germabenzene, cyclic dimetallaalkenes, and fused tricyclic dimetallenes [94–96,128], N–H and O–H bond cleavage catalyzed by single-walled silicon carbide nanotube [98], gold catalyzed cycles [129], the reaction of sulfonyl-containing compounds with ditetrelenes [130], N<sub>2</sub>O activation by substituted disilenes [131], the reaction of disilenes with nitrous oxide [132], and the reactions of phosphino disilenes and their derivatives with an E=E (E = C, Si, Ge, Sn, and Pb) double bond [133]. Alcohols and water [69,134–139], as well as amines [140–146], have been observed to undergo addition reactions with dimer  $\pi$ -bonds on silicon surfaces due to the critical role of reactions at silicon surfaces in disilene chemistry. An investigation of the addition of (2-ethynyl-3-methoxy-2-methylcyclopropyl)benzene to Tip<sub>2</sub>Si=SiTipPh, a disilene with an asymmetric substitution pattern, indicated a step-wise mechanism involving a biradical intermediate based on the regiochemistry of the ring-opened products [147].

### 2.1.3. Reactivity

The calculations, combined with FMO examinations, indicate that two pathways are viable for the reaction of disilene with water, providing the *syn*- and *anti*-products [77,114].

In the model disilene-water addition reaction, the pathway via  $TS_N$  is favored over the pathway via  $TS_E$ , as the energy barrier of  $TS_E$  from  $C_N$  is higher than that of  $TS_N$  from  $C_E$ . The preference for the two pathways in the actual reaction of disilene and silene with various alcohols will depend on the electronic and steric effects of the substituents on the disilene and silene, the nature of the nucleophiles and electrophiles, and other factors [80,83–98,148]. Experimentally, disilenes  $R^*PhSi=SiPhR^*$  ( $R^* = \text{supersilyl} = Si^tBu_3$ ) are yellow, water- and air-sensitive crystals that undergo 1,2-addition with  $H_2O$  to convert to disilanes  $R^*PhHSi-SiOHPhR^*$  [149], where *syn*-addition is preferred to *anti*-addition, as predicted theoretically [77]. Several experimental results on 1,2-addition reactions to disilenes have been reported in the literature [150]. Substituent effects on the reactivity of silenes and digermenes have been investigated experimentally and computationally [151,152]. Additionally, the addition reaction of silenes with alcohols depends on the polarity of the  $Si=C$  bond [153–155].

## 2.2. Unimolecular Rearrangements

Unimolecular or intramolecular rearrangements in organometallic compounds can be categorized into three different types: those proceeding via the breaking and reforming of  $\sigma$ -bonds (sigmatropic rearrangements),  $\pi$ -bonds (haptotropic rearrangements), and both  $\sigma$ - and  $\pi$ -bonds (dyotropic rearrangements) [156]. In sigmatropic rearrangements, the Woodward–Hoffman (W–H) rule [157] dictates that suprafacial 1,3-migration with retention at the migrating center (suprafacial-retention) is symmetry-forbidden, whereas antarafacial-retention and suprafacial-inversion are allowed, though they are usually sterically disfavored. Thermal 1,3-silyl migration in allylic silanes has been experimentally reported by Kwart et al. to proceed concertedly with a symmetry-allowed suprafacial-inversion of the configuration at the migrating silicon (Figure 5), consistent with the W–H rule [158,159]. This experiment led to the long-held belief that the W–H rule for 1,3-migration was valid for silicon systems as well as carbon systems, at least until the development of high-speed and high-performance supercomputers enabled highly reliable *ab initio* MO calculations for large-scale systems.

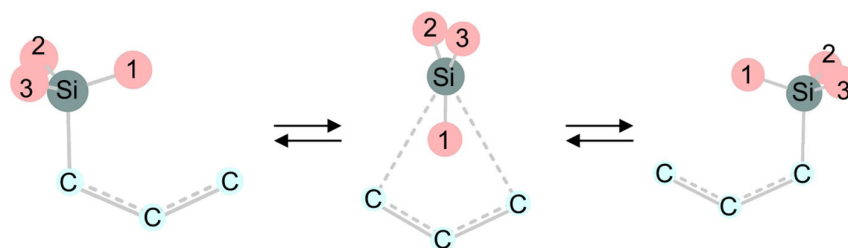


**Figure 5.** 1,3-Silyl migration of allylsilanes with symmetry-allowed suprafacial inversion of configuration at the migrating silicon.

### 2.2.1. 1,3-Sigmatropic Silyl Migration from Carbon to Carbon Featuring High Coordination

Theoretical studies on 1,3-sigmatropic silyl migration of allylsilanes using *ab initio* MO calculations were published simultaneously and independently by two Japanese groups [160,161]. Both concluded impressively that the W–H rule is violated in 1,3-sigmatropic silyl migration of allylsilanes. That is, the symmetry-forbidden suprafacial-retention pathway is preferred to the symmetry-allowed suprafacial-inversion pathway. The stereochemical preference different from Kwart et al.'s findings is likely due to the bulky substituents at silicon in their experiments. Subsequently, experimental evidence of retention stereochemistry in the thermal 1,3-sigmatropic silyl migration of allylic silanes was reported, demonstrating that the stereochemical outcome highly depends on the substitutions at silicon [162]. Carbon-to-carbon 1,3-sigmatropic shifts with retention of the

configuration at the migrating group have also been reported, such as in  $\text{GeCl}_2$  cycloaddition reactions to unsaturated organic compounds [163] and in the interaction process of deactivated silylenes with buta-1,3-diene [164]. The lowest energy pathway in a computational study of the 1,3-sigmatropic rearrangement of 2-vinylsilirane to silacyclopent-3-ene is a symmetry-allowed suprafacial process with inversion of the configuration at the migrating group [165]. A stepwise mechanism may be the dominant reaction pathway in several theoretically studied particular 1,3-sigmatropic rearrangements [166]. A thermal aromatic 1,3-silyl migration was discovered in unprecedented aryne 1,2,3,5-tetrasubstitution by 3-silylaryne and allyl sulfoxides [167].

Theoretical studies of 1,2-migration of H,  $\text{CH}_3$ ,  $\text{CH}=\text{CH}_2$ ,  $\text{SiH}_3$ , and  $\text{GeH}_3$  groups on the P and As atoms indicate that the transition states for the migrations of the methyl and vinyl groups, and the hydrogen atom, are high in energy, while the migration of the groups with the heavier elements of Si and Ge utilizes their hypervalency to have a small activation energy [168]. Kwart et al. proposed an orbital diagram for the 1,3-silyl migration of allylsilane, implicitly assuming a rather unusual trigonal bipyramidal (TBP) transition structure, in which two axial positions at the pentacoordinate silicon are occupied by allyl carbons. The pathway via the TBP transition structure is a suprafacial inversion (Figure 6). Alternatively, the migration could proceed with retention of the configuration at silicon by adopting another pentacoordinate silicon structure, a square pyramidal (SP) structure around the silicon (Figure 6). The pathway via the SP transition structure is suprafacial retention. In the calculations, the two suprafacial pathways with different stereochemical configurations at silicon were indeed obtained.

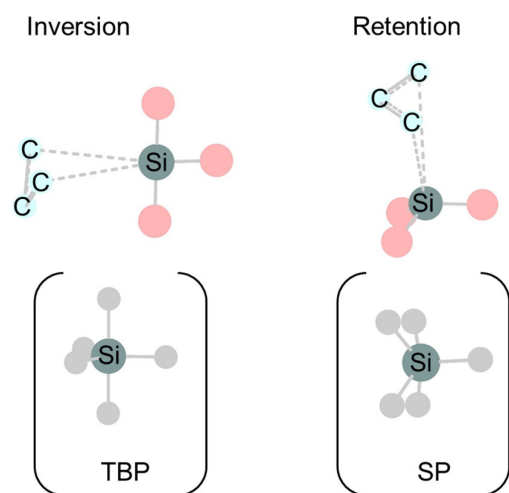


**Figure 6.** The trigonal bipyramidal (TBP) and square pyramidal (SP) transition structures in 1,3-sigmatropic silyl migration of allylsilanes.

Examining the interactions between silyl and aryl radicals in the transition structures qualitatively reveals the retention preferences (Figure 7). The LUMO, SOMO (singly occupied molecular orbital), and HOMO of the allyl radical are anti-bonding, non-bonding, and bonding orbitals, respectively. The LUMO and SOMO of the silyl radicals involved in the interaction are the same for both the TBP and SP transition structures, i.e., the p-orbitals parallel and perpendicular to the allylic chain, respectively. The HOMO of the silyl radical differs between the TBP and SP transition structures, being the p-orbital perpendicular and parallel to the allyl radical chain, respectively. The major stabilization of the TBP transition structure for suprafacial-inversion is caused by the interaction between the low-lying LUMO of the silyl radical with the non-bonding SOMO of the allyl radical, as predicted by the W–H rule. On the other hand, due to the difference in HOMO, in case of

the SP transition structure for suprafacial-retention, in addition to the stabilization by the interaction of the low-lying LUMO of the silyl radical with the non-bonding SOMO of the allyl radical, there is also stabilization by the interaction of the subjacent bonding orbital of the allyl radical with the SOMO of the silyl radical.

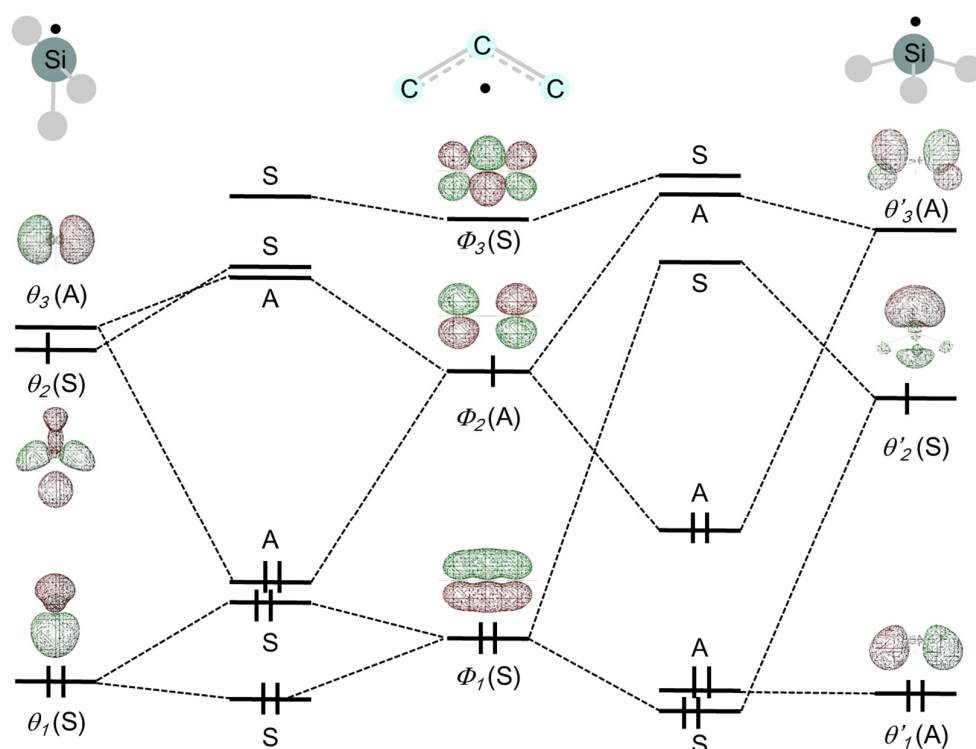


**Figure 7.** Interaction diagram of frontier orbitals in TBP and SP transition structures for 1,3-silyl migration of allylsilanes. The frontier orbitals of the silyl and allyl radicals interacting in the transition structures are constructed by the three  $\pi$  orbitals ( $\phi_1$ ,  $\phi_2$ , and  $\phi_3$ ) of the allyl radical and the three 3p orbitals ( $\theta_1$ ,  $\theta_2$ , and  $\theta_3$ ) or ( $\theta'_1$ ,  $\theta'_2$ , and  $\theta'_3$ ) of the silyl radical. The symmetry notations S (symmetric) and A (antisymmetric) refer to the planes that bisect the allyl CCC plane.

### 2.2.2. 1,3-Silyl Migration Between Heteroatoms

It has been established that intramolecular thermal 1,3-sigmatropic silyl migration occurs concertedly from carbon to carbon in allylic silanes [158,159] and between heteroatoms in silylmethyl ketones [169] with optical active silyl groups. The latter migration in silylmethyl ketones is known as the Brook rearrangement. These migrations were considered to be mechanically distinguished by a striking difference in stereochemical outcome. That is, 1,3-silyl migration in allylic silanes occurs with inversion stereochemistry, whereas in silylmethyl ketones it occurs with retention stereochemistry. However, theoretical studies by Takahashi et al. [160] and Yamabe et al. [161] revealed, as mentioned in Section 2.2.1, that two concerted pathways leading to retention and inversion in silicon are both allowed for thermal 1,3-silyl migration in allylsilanes, with the retention pathway being lower in energy. These reports on retention preference in the thermal 1,3-silyl migration of allylsilane stimulated further the theoretical investigations into the mechanism of 1,3-silyl migration in silylmethyl ketones.

In the theoretical study of concerted 1,3-silyl migration in formylmethylsilane, the calculated activation energy, as well as retention stereochemistry, are in good agreement with experimental results for silylmethyl ketones [170]. 1,3-Silyl migration in both allylsilane and formylmethylsilane proceeds concertedly, without the formation of intermediates, via a four-membered cyclic transition structure, with retention stereochemistry around the silicon. However, there are essential differences in the transition structures. 1,3-Silyl migration

with retention in formylmethylsilane is best explained as an intramolecular nucleophilic substitution at silicon, whereas the corresponding migration in allylsilanes is characterized as an electrocyclic sigmatropic rearrangement controlled by subjacent orbital interactions [171,172]. Reaction pathways involving 1,3-silyl migration between heteroatoms have been reported computationally and experimentally in various reactions [173–186]. In the benzidine rearrangement, an unprecedented suprafacial symmetry-allowed 1,3-sigmatropic shift from nitrogen to carbon with an inversion of the configuration at the migrating nitrogen atom was supported by a systematic investigation of experiments and theoretical calculations [187].

### 3. Photochemical Reactions

The complete active space self-consistent field (CASSCF) method is one of the most appropriate ab initio methods for investigating the reaction pathways on excited states. Since Bernardi et al. reported on the photochemical sigmatropic rearrangement of but-1-ene [188], several photochemical reactions have been extensively studied for carbon systems using the CASSCF method [189–198]. It is commonly understood that photochemical investigations using the CASSCF method require a careful selection of the correct orbitals for active space. With adequately selected orbitals for the active space and a sufficiently large basis set, the excitation energies calculated at the MP2-CAS level are in excellent agreement with the experimentally observed UV absorption maxima [199]. In addition to the ones presented here, theoretical studies on the photochemical reactions of organosilicon compounds using the CASSCF method have been published [200–202].

Full photodynamics calculations are prohibitively expensive for all but the smallest molecules, unless simplifying approximations are employed. Time-dependent DFT (TDDFT) offers a promising and relatively inexpensive alternative to more accurate, but costly, quantum chemical approaches, for on-the-fly calculations of excitation energies [203,204]. Several applications of TDDFT to photochemical reactions in silicon chemistry are documented in the literature, primarily focusing on the investigation of solid-state materials such as crystals, surfaces, two-dimensional materials, and nanomaterials [205–209].

#### 3.1. Interconversion

Cyclopropenylidene (**1**,  $c\text{-C}_3\text{H}_2$ ) is abundant in molecular clouds of interstellar space and plays a decisive role in the chemistry of interstellar clouds [210–213]. The silicon analog, silacyclopropenylidene (**3**,  $c\text{-C}_2\text{H}_2\text{Si}$ ), also appears to be of interest, especially in astrochemistry and structural chemistry [214]. Maier et al. reported the synthesis and photoisomerization of **1** and **3** [215,216]. It was shown that the photochemical interconversion of **1** occurs between three  $\text{C}_3\text{H}_2$  isomers: **1**, propargylene (**2**), and vinylidenecarbene [215]. On the other hand, the photochemical reaction of **3** is more complex, with several isomers detected during the reaction [216]. The reaction products detected by infrared spectroscopy are **2** and ethynylsilylene (**4**), upon irradiation with 254 nm light [215] for **1** and 313 nm light for **3** [216], respectively (Figure 8). Recently, crossed beam experiments and computational studies have revealed a synthetic route to singlet **4** ( $\text{HCCSiH}$ ;  $X^1A'$ ) [217]. The ground-state structures, energetics, and vibrational frequencies observed in photochemical reactions of **1**, **3**, the germanium analog ( $\text{GeC}_2\text{H}_2$ ),  $\text{SiC}_4\text{H}_2$  isomers, and  $\text{Si}_2\text{C}_5\text{H}_2$  isomers have been intensively investigated by theoretical chemists [218–228].

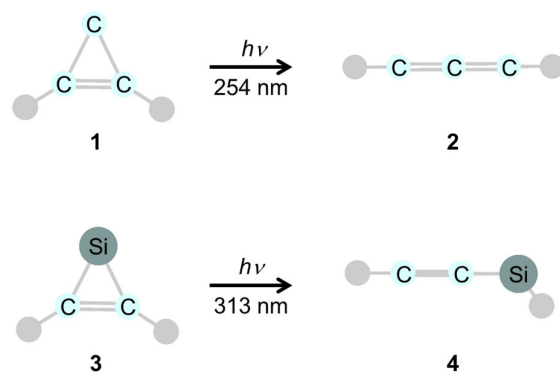


**Figure 8.** Photochemical reactions of cyclopropenyldiene (1) and silacyclopropenyldiene (3).

The photochemical reaction pathway of **3** has been investigated in detail by Takahashi et al. using the CASSCF method [199]. The excited state through which the photochemical reaction proceeds was carefully chosen because the forbidden state  $^1(\sigma_{\text{SiC}} \rightarrow 3\text{p})$  is energetically close to the allowed state,  $^1(\text{n} \rightarrow 3\text{p})$ . For examining the orbitals and planning the active space, the natural orbitals are examined. Then, one  $\pi_{\text{CC}}$  and two  $\sigma_{\text{SiC}}$  orbitals, and one lone-pair orbital at silicon are selected. The use of the eight active orbitals to describe the present system is justified as follows: The photochemical reaction treated here is the Si–C bond cleavage. The first allowed band is best described as  $\text{n} \rightarrow 3\text{p}(\text{Si})$ . The carbon  $\pi$  orbital ( $\pi_{\text{CC}}$ ) is mixed in an antibonding manner with the  $3\text{p}(\text{Si})$  orbital. The photochemical reaction from the  $\text{S}_1$   $^1(\text{n} \rightarrow 3\text{p})$  excited state of *c*- $\text{C}_2\text{H}_2\text{Si}$  leads to an  $\text{S}_1/\text{S}_0$  conical intersection (CI), and the photoexcited state decays nonradiatively to  $\text{S}_0$ . Relaxation on the  $\text{S}_1$  surface leads to the cleavage of the C–Si single bond, followed by hydrogen migration from carbon to silicon with ring opening in the dark reaction.

### 3.2. Sigmatropic Rearrangement

Photochemical 1,3-silyl migration is of particular interest from a mechanistic perspective. Numerous reactions involving photochemical silyl migration from carbon to carbon [229,230] or between heteroatoms [231–245] have been reported in the literature. However, the stereochemical and mechanistic details have rarely been described [230]. The stereochemistry of 1,3-sigmatropic rearrangements is systematically explained by the well-established Woodward–Hoffmann (W–H) rules based on orbital symmetry [157]. In photochemical 1,3-sigmatropic rearrangements, the migrating group moves according to a supra process and retains its configuration, whereas thermal suprafacial rearrangements occur with inversion of configuration at the migrating center (Figure 5). While the W–H rule correctly predicts the stereochemistry in reactions of organic compounds with a carbon framework, it is of great interest to investigate whether this rule can be applied to the stereoselection of organosilicon compounds. According to modern experiments and quantum chemical calculations, low-lying crossings on the potential energy surface (conical intersection: CI) are a common feature of excited states relevant for photochemical reactions.

An experimental study of the photochemical 1,3-silyl migration in allylsilanes was reported by Kira et al. in 1989 [230]. The photochemical migration occurs with inversion of the silyl configuration, contrary to the W–H rules. The configuration of the photochemical products was identified by performing a thermal reverse reaction that occurs with inversion, according to Kwart et al. [158,159]. On the other hand, the thermal 1,3-silyl migration of allylic silanes with inversion of the configuration was doubted by Brook [246]. Furthermore, theoretical studies have shown that the thermal 1,3-silyl migration of allylsilanes favors retention of configuration [160,161], and experiments with stereochemically rigid 4-*tert*-butylsilacyclohexane derivatives support the preference for retention [162].

The photochemical 1,3-silyl rearrangement of allylsilanes has been theoretically investigated by Takahashi [247], focusing on stereochemistry and reaction mechanism. To select the correct orbitals for the active space in the photochemical investigation using the CASSCF methods, the natural orbitals are examined, and the six active orbitals are selected: the  $\pi$ -,  $\pi^*$ -,  $\sigma$ -, and  $\sigma^*$ -orbitals in the C=C bond and the  $\sigma$ - and  $\sigma^*$ -orbitals in the Si-C bond that is cleaved. In the system with a complete active space comprising six electrons in six orbitals, denoted by CAS(6,6), two electrons among six are fully coupled in a  $\sigma_{CC}$  bond, leaving two possible spin couplings for the remaining four electrons. The driving force that controls the generation of ground-state photoproducts is expected to be provided by recoupling these four electrons in the partly fragmented bonds that occur when the system decays. The use of six active orbitals is justified as follows: For the description of the photochemical 1,3-sigmatropic shifts in a carbon system, four electrons in four orbitals, denoted by CAS(4,4), is the usual active space, as reported by Bernardi et al. [188]. However, better Si-C bond lengths, related to the possibility of the dissociation of an allyl group, are given in CAS(6,6) than in CAS(4,4).

The stereochemistry of the photochemical 1,3-silyl rearrangement of allylsilanes was theoretically confirmed to be retained, in agreement with the W-H rule [247]. The calculated CI structure is consistent with ubiquitous control elements (Figure 9) in photochemical sigmatropic rearrangements within the carbon framework [194], indicating the possibility of a dissociation pathway to radicals, in addition to the 1,3-shift pathway. Fifteen years after Takahashi's theoretical work [247], Hammer et al. reported experimentally a stereoselective photochemical 1,3-sigmatropic silyl shift and the existence of a silyl/allyl CIs [248].

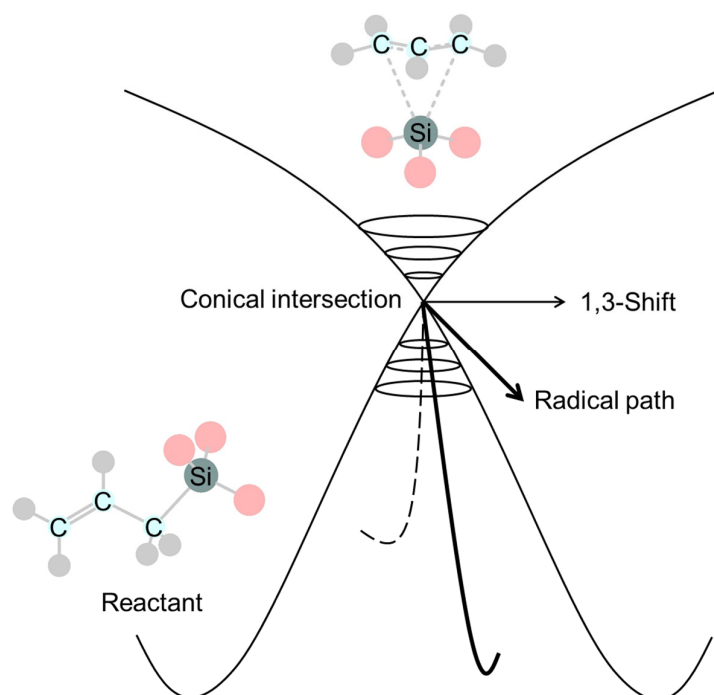


**Figure 9.** A characteristic conical intersection (CI) structure common to photochemical sigmatropic shifts reported as a ubiquitous control element [194].

#### 4. Conclusions

In this review article, we introduce the theoretical studies on the thermal and photochemical reactions of organosilicon compounds, focusing on our work conducted in 1997–2005. We also comprehensively introduce the related experimental and theoretical studies by previous and recent researchers. In the late 1980s, thermal reactions of unsaturated silicon compounds could be treated with quantitative accuracy using *ab initio*

MO calculations without experimental parameters, allowing for the theoretical prediction of reaction path preferences. Furthermore, the development of high-performance and high-speed supercomputers has accelerated the ab initio MO calculations of larger molecules, containing heavier elements such as silicon. In particular, a frequency analysis to distinguish between the transition states and local minima, which are essential for investigating reaction pathways, required time-consuming, large-scale calculations. Theoretical studies of photochemical reactions started a little bit later and still continue to intrigue theoretical chemists, with recent advances in experimental techniques to capture photochemical reactions.

**Funding:** This research received no external funding.

**Data Availability Statement:** No new data were created or analyzed in this study. Data sharing is not applicable to this article.

**Conflicts of Interest:** The author declares no conflicts of interest.

## References

1. Vogt, P.; Padova, P.D.; Quaresima, C.; Avila, J.; Frantzeskakis, E.; Asensio, M.C.; Resta, A.; Ealet, B.; Lay, G.L. Silicene: Compelling experimental evidence for graphenelike two-dimensional silicon. *Phys. Rev. Lett.* **2012**, *108*, 155501. [[CrossRef](#)] [[PubMed](#)]
2. Feng, B.; Ding, Z.; Meng, S.; Yao, Y.; He, X.; Cheng, P.; Chen, L.; Wu, K. Evidence of silicene in honeycomb structures of silicon on Ag(111). *Nano Lett.* **2012**, *12*, 3507–3511. [[CrossRef](#)] [[PubMed](#)]
3. Gao, J.; Zhao, J. Initial geometries, interaction mechanism and high stability of silicene on Ag(111) surface. *Sci. Rep.* **2012**, *2*, 861. [[CrossRef](#)] [[PubMed](#)]
4. Kaltsas, D.; Tsetseris, L.; Dimoulas, A. Structural evolution of single-layer films during deposition of silicon on silver: A first principles study. *J. Phys. Condens. Matter* **2012**, *24*, 442001. [[CrossRef](#)]
5. Guo, Z.-X.; Furuya, S.; Iwata, J.-I.; Oshiyama, A. Absence and presence of Dirac electrons in silicene on substrates. *Phys. Rev. B* **2013**, *87*, 235435. [[CrossRef](#)]
6. Wang, Y.-P.; Cheng, H.-P. Absence of a Dirac cone in silicene on Ag(111): First-principles density functional calculations with a modified effective band structure technique. *Phys. Rev. B* **2013**, *87*, 245430. [[CrossRef](#)]
7. Tsoutsou, D.; Xenogiannopoulou, E.; Golias, E.; Tsipas, P.; Dimoulas, A. Evidence for hybrid surface metallic band in (4 × 4) silicene on Ag(111). *Appl. Phys. Lett.* **2013**, *103*, 231604. [[CrossRef](#)]
8. Moras, P.; Mentis, T.O.; Sheverdyeva, P.M.; Locatelli, A.; Carbone, C. Coexistence of multiple silicene phases in silicon grown on Ag(111). *J. Phys. Condens. Matter* **2014**, *26*, 185001. [[CrossRef](#)]
9. Feng, Y.; Liu, D.; Feng, B.; Liu, X.; Zhao, L.; Xie, Z.; Liu, Y.; Liang, A.; Hu, C.; Hu, Y.; et al. Direct evidence of interaction-induced Dirac cones in a monolayer silicene/Ag(111) system. *Proc. Natl. Acad. Sci. USA* **2016**, *113*, 14656–14661. [[CrossRef](#)]
10. Du, Y.; Zhuang, J.; Wang, J.; Li, Z.; Liu, H.; Zhao, J.; Xu, X.; Feng, H.; Chen, L.; Wu, K.; et al. Quasi-freestanding epitaxial silicene on Ag(111) by oxygen intercalation. *Sci. Adv.* **2016**, *2*, e1600067. [[CrossRef](#)]
11. Fleurence, A.; Friedlein, R.; Ozaki, T.; Kawai, H.; Wang, Y.; Yamada-Takamura, Y. Experimental evidence for epitaxial silicene on diboride thin films. *Phys. Rev. Lett.* **2012**, *108*, 245501. [[CrossRef](#)] [[PubMed](#)]
12. Meng, L.; Wang, Y.; Zhang, L.; Du, S.; Wu, R.; Li, L.; Zhang, Y.; Li, G.; Zhou, H.; Hofer, W.A.; et al. Buckled silicene formation on Ir(111). *Nano Lett.* **2013**, *13*, 685–690. [[CrossRef](#)] [[PubMed](#)]
13. Chiappe, D.; Scalise, E.; Cinquanta, E.; Grazianetti, C.; van den Broek, B.; Fanciulli, M.; Houssa, M.; Molle, A. Two-dimensional Si nanosheets with local hexagonal structure on a MoS<sub>2</sub> surface. *Adv. Mater.* **2014**, *26*, 2096–2101. [[CrossRef](#)] [[PubMed](#)]
14. Brumfiel, G. Sticky problem snares wonder material. *Nature* **2013**, *495*, 152–153. [[CrossRef](#)]
15. West, R.; Fink, M.J.; Michl, J. Tetramesityldisilene, a stable compound containing a silicon–silicon double bond. *Science* **1981**, *214*, 1343–1344. [[CrossRef](#)]
16. Sekiguchi, A.; Kinjo, R.; Ichinohe, M. A stable compound containing a silicon-silicon triple bond. *Science* **2004**, *305*, 1755–1757. [[CrossRef](#)]
17. Ishida, S.; Iwamoto, T.; Kabuto, C.; Kira, M. A stable silicon-based allene analogue with a formally *sp*-hybridized silicon atom. *Nature* **2003**, *421*, 725–727. [[CrossRef](#)]
18. Kira, M. Isolable silylene, disilenes, trisilaallene, and related compounds. *J. Organomet. Chem.* **2004**, *689*, 4475–4488. [[CrossRef](#)]
19. Bejan, I.; Güclü, D.; Inoue, S.; Ichinohe, M.; Sekiguchi, A.; Scheschkewitz, D. Stable cyclic silenes from reaction of disilenides with carboxylic acid chlorides. *Angew. Chem. Int. Ed.* **2007**, *46*, 3349–3352. [[CrossRef](#)]

20. Smit, C.N.; Lock, F.M.; Bickelhaupt, F. 2,4,6-Tri-*tert*-butylphenylphosphene-dimesitylsilene; the first phosphasilaalkene. *Tetrahedron Lett.* **1984**, *25*, 3011–3014. [[CrossRef](#)]
21. Smit, C.N.; Bickelhaupt, F. Phosphasilenes: Synthesis and spectroscopic characterization. *Organometallics* **1987**, *6*, 1156–1163. [[CrossRef](#)]
22. Niecke, E.; Klein, E.; Nieger, M. Synthesis, structure, and reactivity of a 1,3-diphospha-2-silaallyl anion. *Angew. Chem. Int. Ed. Engl.* **1989**, *28*, 751–752. [[CrossRef](#)]
23. Driess, M.; Rell, S.; Pritzkow, H. First structural characterization of silicon–arsenic and silicon–phosphorus multiple bonds in silylated silylidene-arsanes and -phosphanes; X-ray structure of a tellura-arsasilirane derivative. *J. Chem. Soc. Chem. Commun.* **1995**, *2*, 253–254. [[CrossRef](#)]
24. Lange, D.; Klein, E.; Bender, H.; Niecke, E.; Nieger, M.; Pietschnig, R.; Schoeller, W.W.; Ranaivonjatovo, H. 1,3-Diphospha-2-silaallylic lithium complexes and anions: Synthesis, crystal structures, reactivity, and bonding properties. *Organometallics* **1998**, *17*, 2425–2432. [[CrossRef](#)]
25. Appel, R.; Fölling, P.; Josten, B.; Siray, M.; Winkhaus, V.; Knoch, F. Phosphaallenes. *Angew. Chem. Int. Ed. Engl.* **1984**, *23*, 619–620. [[CrossRef](#)]
26. Karsch, H.H.; Reisacher, H.-U.; Müller, G. Molecular structure of a 1,3-diphosphaallene: (2,4,6-*t*Bu<sub>3</sub>C<sub>6</sub>H<sub>2</sub>)P=C=P(2,4,6-*t*Bu<sub>3</sub>C<sub>6</sub>H<sub>2</sub>), a phosphorus analogue of carbon disulfide. *Angew. Chem. Int. Ed. Engl.* **1984**, *23*, 618–619. [[CrossRef](#)]
27. Appel, R.; Winkhaus, V.; Knoch, F. Low coordinated phosphorus-compounds. 48. Synthesis of 1-phosphaallenes. *Chem. Ber. Recl.* **1986**, *119*, 2466–2472. [[CrossRef](#)]
28. Märkl, G.; Herold, U. 1-Phospha-1,2-butadiene-1-phospha-1,2,3-butatriene. *Tetrahedron Lett.* **1988**, *29*, 2935–2938. [[CrossRef](#)]
29. Märkl, G.; Reitingner, S. 3H-phosphaallen-alkinyl-1H-phosphan-tautomere. *Tetrahedron Lett.* **1988**, *29*, 463–466. [[CrossRef](#)]
30. Märkl, G.; Kreitmeier, P. 1,4-Diphospha-butatriene. *Angew. Chem. Int. Ed. Engl.* **1988**, *27*, 1360–1361. [[CrossRef](#)]
31. Yoshifuji, M.; Toyota, K.; Niitsu, T.; Inamoto, N.; Okamoto, Y.; Aburatani, R. The first separation of an optically active 1,3-diphospha-allene of axial dissymmetry. *J. Chem. Soc. Chem. Commun.* **1986**, *20*, 1550–1551. [[CrossRef](#)]
32. Yoshifuji, M.; Sasaki, S.; Inamoto, N. A new direct method for introducing 2-(2,4,6-tri-*t*-butylphenyl)-2-phosphavinylidene group. Formation of 1-phospha- and 1,3-diphospha-allenes. *Tetrahedron Lett.* **1989**, *30*, 839–842. [[CrossRef](#)]
33. Yoshifuji, M.; Sasaki, S.; Inamoto, N. The first preparation of an unsymmetrical 1,3-diphospha-allene carrying 2,4,6-tri-*t*-butylphenyl and 2,4,6-tri-*t*-pentylphenyl as protecting groups. *J. Chem. Soc. Chem. Commun.* **1989**, *22*, 1732–1733. [[CrossRef](#)]
34. Yoshifuji, M.; Niitsu, T.; Shiomi, D.; Inamoto, N. A versatile preparation of 2,6-di-*t*-butylbromobenzene. Application to steric protection for organophosphorus compounds in low coordination states. *Tetrahedron Lett.* **1989**, *30*, 5433–5436. [[CrossRef](#)]
35. Miracle, G.E.; Ball, J.L.; Powell, D.R.; West, R. The first stable 1-silaallene. *J. Am. Chem. Soc.* **1993**, *115*, 11598–11599. [[CrossRef](#)]
36. Trommer, M.; Miracle, G.E.; Eichler, B.E.; Powell, D.R.; West, R. Synthesis and reactivity of several stable 1-silaallenes. *Organometallics* **1997**, *16*, 5737–5747. [[CrossRef](#)]
37. Eichler, B.; West, R. Chemistry of group 14 heteroallenes. *Adv. Organomet. Chem.* **2001**, *46*, 1–46.
38. Eichler, B.E.; Miracle, G.E.; Powell, D.R.; West, R. Three stable 1-silapropadienes. *Main Group Met. Chem.* **1999**, *22*, 147–162. [[CrossRef](#)]
39. Iwamoto, T.; Abe, T.; Kabuto, C.; Kira, M. A missing allene of heavy group 14 elements: 2-germadisilaallene. *Chem. Commun.* **2005**, *41*, 5190–5192. [[CrossRef](#)]
40. Iwamoto, T.; Masuda, H.; Kabuto, C.; Kira, M. Trigermaallene and 1,3-digermasilaallene. *Organometallics* **2005**, *24*, 197–199. [[CrossRef](#)]
41. Rigon, L.; Ranaivonjatovo, H.; Escudié, J.; Dubourg, A.; Declercq, J.P. ArP=C=Si(Ph)Tip: The first allenic compound with doubly bonded phosphorus and silicon. *Chem. Eur. J.* **1999**, *5*, 774–781. [[CrossRef](#)]
42. Berger, D.J.; Gaspar, P.P.; Grev, R.S.; Mathey, F. Molecular orbital study of the vinylphosphinidene to phosphapropyne rearrangement. *Organometallics* **1994**, *13*, 640–646. [[CrossRef](#)]
43. Gordon, M.S.; Koob, R.D. Relative stability of multiple bonds to silicon: An ab initio study of C<sub>2</sub>SiH<sub>4</sub> isomers. *J. Am. Chem. Soc.* **1981**, *103*, 2939–2944. [[CrossRef](#)]
44. Maier, G.; Pacl, H.; Reisenauer, H.P. Silacyclopropene: Generation by high-vacuum flash pyrolysis and matrix-spectroscopic identification. *Angew. Chem. Int. Ed. Engl.* **1995**, *34*, 1439–1441. [[CrossRef](#)]
45. Barthelat, J.-C.; Trinquier, G.; Bertrand, G. Theoretical investigations on some C<sub>2</sub>SiH<sub>4</sub> isomers. *J. Am. Chem. Soc.* **1979**, *101*, 3785–3789. [[CrossRef](#)]
46. Lien, M.H.; Hopkinson, A.C. An ab initio molecular orbital study of ten isomers on the C<sub>2</sub>SiH<sub>4</sub> energy surface. *Chem. Phys. Lett.* **1981**, *80*, 114–118. [[CrossRef](#)]
47. Nguyen, M.T.; Vansweevelt, H.; Vanquickenborne, L.G. Remarkable effect of fluorine and chlorine atoms on the stability of 1H-phosphirene. *Chem. Ber.* **1992**, *125*, 923–927. [[CrossRef](#)]
48. Veszprémi, T.; Petrov, K.; Nguyen, C.T. From silaallene to cyclotrisilanylidene. *Organometallics* **2006**, *25*, 1480–1484. [[CrossRef](#)]

49. Pietschnig, R.; Orthaber, A. The relative stabilities of 1,3-diphospha-2-silaallene and some of Its isomers. *Eur. J. Inorg. Chem.* **2006**, *2006*, 4570–4576. [[CrossRef](#)]
50. Schoeller, W.W. van der Waals interactions in sterically crowded disilenes. *J. Mol. Struct. THEOCHEM* **2010**, *957*, 66–71. [[CrossRef](#)]
51. Karni, M.; Apeloig, Y. Substituent effects on the geometries and energies of the Si=Si double bond. *J. Am. Chem. Soc.* **1990**, *112*, 8589–8590. [[CrossRef](#)]
52. Takahashi, M.; Kawazoe, Y. Metal-substituted disilynes with linear form. *Organometallics* **2008**, *27*, 4829–4832. [[CrossRef](#)]
53. Kosa, M.; Karni, M.; Apeloig, Y. How to design linear allenic-type trisilaallenes and trigermaallenes. *J. Am. Chem. Soc.* **2004**, *126*, 10544–10545. [[CrossRef](#)] [[PubMed](#)]
54. Takahashi, M.; Kawazoe, Y. Theoretical study on planar anionic polysilicon chains and cyclic Si<sub>6</sub> anions with D<sub>6h</sub> symmetry. *Organometallics* **2005**, *24*, 2433–2440. [[CrossRef](#)]
55. Takahashi, M.; Kawazoe, Y. Theoretical proposal of planar silicon oligomer and silicon benzene. *Comput. Mater. Sci.* **2006**, *36*, 30–35. [[CrossRef](#)]
56. Takahashi, M. Flat building blocks for flat silicone. *Sci. Rep.* **2017**, *7*, 10855. [[CrossRef](#)]
57. Takahashi, M. Flat zigzag silicene nanoribbon with Be bridge. *ACS Omega* **2021**, *6*, 12099–12104. [[CrossRef](#)]
58. Takahashi, M. Polysilyne chains bridged with beryllium lead to flat 2D Dirac materials. *Sci. Rep.* **2023**, *13*, 13182. [[CrossRef](#)]
59. Takahashi, M. Polyanionic hexagons: X<sub>6</sub><sup>n−</sup> (X = Si, Ge). *Symmetry* **2010**, *2*, 1745–1762. [[CrossRef](#)]
60. Okazaki, R.; West, R. Chemistry of stable disilenes. *Adv. Organomet. Chem.* **1996**, *39*, 231–273.
61. West, R. The disilenes: Chemistry of silicon-silicon double bonds. *Pure Appl. Chem.* **1984**, *56*, 163–173. [[CrossRef](#)]
62. Raabe, G.; Michl, J. Multiple bonding to silicon. *Chem. Rev.* **1985**, *85*, 419–509. [[CrossRef](#)]
63. West, R. Chemistry of the silicon–silicon double bond. *Angew. Chem. Int. Ed. Engl.* **1987**, *26*, 1201–1211. [[CrossRef](#)]
64. Raabe, G.; Michl, J. Multiple bonds to silicon. In *Organic Silicon Compounds*; Patai, S., Rappoport, Z., Eds.; John Wiley & Sons, Ltd.: Chester, UK, 1989; Volume 1, Chapter 17; pp. 1015–1142. [[CrossRef](#)]
65. Tsumuraya, T.; Batcheller, S.A.; Masamune, S. Strained-ring and double-bond systems consisting of the group-14 elements Si, Ge, and Sn. *Angew. Chem. Int. Ed. Engl.* **1991**, *30*, 902–930. [[CrossRef](#)]
66. Grev, R.S. Structure and bonding in the parent hydrides and multiply bonded silicon and germanium compounds: From Mh<sub>n</sub> to R<sub>2</sub>M=M'R<sub>2</sub> and RM≡M'R. *Adv. Organomet. Chem.* **1991**, *33*, 125–170. [[CrossRef](#)]
67. Kira, M.; Iwamoto, T. Stable cyclic and acyclic persilyldisilenes. *J. Organomet. Chem.* **2000**, *611*, 236–247. [[CrossRef](#)]
68. Kira, M.; Ishima, T.; Iwamoto, T.; Ichinohe, M. A mechanistic study of reactions of stable disilenes with haloalkanes. *J. Am. Chem. Soc.* **2001**, *123*, 1676–1682. [[CrossRef](#)]
69. Eng, J.; Raghavachari, K.; Struck, L.M.; Chabal, Y.J.; Bent, B.E.; Flynn, G.W.; Christman, S.B.; Chaban, E.E.; Williams, G.P.; Radermacher, K.; et al. A vibrational study of ethanol adsorption on Si(100). *J. Chem. Phys.* **1997**, *106*, 9889–9898. [[CrossRef](#)]
70. Wiberg, N.; Wagner, G.; Müller, G.; Riede, J. Unsaturated silicon compounds. VII. Preparation and structure of a silaethene tetrahydrofuranate. *J. Organomet. Chem.* **1984**, *271*, 381–391. [[CrossRef](#)]
71. Wiberg, N. Unsaturated compounds of silicon and group homologues. VIII. Unsaturated silicon and germanium compounds of the types R<sub>2</sub>E=C(SiR<sub>3</sub>)<sub>2</sub> and R<sub>2</sub>E=N(SiR<sub>3</sub>)<sub>3</sub> (E = Si, Ge). *J. Organomet. Chem.* **1984**, *273*, 141–177. [[CrossRef](#)]
72. Leigh, W.J.; Sluggett, G.W. Aryldisilane photochemistry. Substituent and solvent effects on the photochemistry of arylidisilanes and the reactivity of 1,3,5-(1-sila)hexatrienes. *Organometallics* **1994**, *13*, 269–281. [[CrossRef](#)]
73. Bradaric, C.J.; Leigh, W.J. Substituent effects on the reactivity of the silicon–carbon double bond. Mechanistic studies of the ene-addition of acetone to reactive arylsilenes. *Organometallics* **1998**, *17*, 645–651. [[CrossRef](#)]
74. Leigh, W.J.; Bradaric, C.J.; Sluggett, G.W. 1,1-Diphenylsilene. *J. Am. Chem. Soc.* **1993**, *115*, 5332–5333. [[CrossRef](#)]
75. Bradaric, C.J.; Leigh, W.J. Arrhenius parameters for the addition of nucleophiles to the silicon–carbon double bond of 1,1-diphenylsilene. *J. Am. Chem. Soc.* **1996**, *118*, 8971–8972. [[CrossRef](#)]
76. Bradaric, C.J.; Leigh, W. Substituent effects on the reactivity of the silicon–carbon double bond. Arrhenius parameters for the reaction of 1,1-diarylsilenes with alcohols and acetic acid. *J. Can. J. Chem.* **1997**, *75*, 1393–1402. [[CrossRef](#)]
77. Takahashi, M.; Veszprémi, T.; Hajgató, B.; Kira, M. Theoretical study on stereochemical diversity in the addition of water to disilene. *Organometallics* **2000**, *19*, 4660–4662. [[CrossRef](#)]
78. De Young, D.J.; Fink, M.J.; West, R. The Addition reactions of two disilenes. *Main Group Met. Chem.* **1987**, *10*, 19–43.
79. Sekiguchi, A.; Maruki, I.; Sakurai, H. Regio- and stereochemistry and kinetics in the addition-reactions of alcohols to phenyl-substituted disilens. *J. Am. Chem. Soc.* **1993**, *115*, 11460–11466. [[CrossRef](#)]
80. Apeloig, Y.; Nakash, M. Solvent-dependent stereoselectivity in the addition of *p*-CH<sub>3</sub>OC<sub>6</sub>H<sub>4</sub>OH to (*E*)-1,2-di-*tert*-butyl-1,2-dimesityldisilene. Evidence for rotation around the Si–Si bond in the zwitterionic intermediate. *Organometallics* **1998**, *17*, 1260–1265. [[CrossRef](#)]
81. Fukui, K. Recognition of stereochemical paths by orbital interaction. *Acc. Chem. Res.* **1971**, *4*, 57–64. [[CrossRef](#)]
82. Fleming, I. *Frontier Orbitals and Organic Chemical Reactions*; Wiley: London, UK, 1976.

83. Veszprémi, T.; Takahashi, M.; Hajgató, B.; Kira, M. The mechanism of 1,2-addition of disilene and silene. 1. Water and alcohol addition. *J. Am. Chem. Soc.* **2001**, *123*, 6629–6638. [[CrossRef](#)] [[PubMed](#)]
84. Hajgató, B.; Takahashi, M.; Kira, M.; Veszprémi, T. The mechanism of 1,2-addition of disilene and silene: Hydrogen halide addition. *Chem. Eur. J.* **2002**, *8*, 2126–2133. [[CrossRef](#)] [[PubMed](#)]
85. Takahashi, M.; Veszprémi, T.; Kira, M. 1,2-Addition reaction of monosubstituted disilenes: An ab initio study. *Organometallics* **2004**, *23*, 5768–5778. [[CrossRef](#)]
86. Takahashi, M.; Veszprémi, T.; Sakamoto, K.; Kira, M. Role of initial complexes in 1,2-addition reactions of disilene derivatives. *Mol. Phys.* **2002**, *100*, 1703–1712. [[CrossRef](#)]
87. Bendikov, M.; Quadt, S.R.; Rabin, O.; Apeloig, Y. Addition of nucleophiles to silenes. A theoretical study of the effect of substituents on their kinetic stability. *Organometallics* **2002**, *21*, 3930–3939. [[CrossRef](#)]
88. Su, M.-D. Theoretical study of the reaction mechanism of abstraction reactions of disilenes and digermenes with haloalkanes. *J. Phys. Chem. A* **2004**, *108*, 823–832. [[CrossRef](#)]
89. Su, M.-D. Mechanism of abstraction reactions of dimetallenes ( $R_2X = XR_2$ ; X = C, Si, Ge, Sn, Pb) with halocarbons: A theoretical study. *Inorg. Chem.* **2004**, *43*, 4846–4861. [[CrossRef](#)]
90. Wang, Y.; Zeng, X. Theoretical study on the addition reactions of MeOH, PhOH and PhSH to silastannenes. *Comput. Theor. Chem.* **2015**, *1058*, 12–20. [[CrossRef](#)]
91. Wang, Y.; Zeng, X. Addition reactions of H<sub>2</sub>O to germastannenes: A computational study. *Russ. J. Phys. Chem. A* **2018**, *92*, 1699–1705. [[CrossRef](#)]
92. Wang, Y.; Zeng, X. Comparative theoretical study on the reactivity of digermenes and disilenes in addition reactions. *Russ. J. Phys. Chem. A* **2020**, *94*, 800–805. [[CrossRef](#)]
93. McOnie, S.L.; Özpınar, G.A.; Bourque, J.L.; Müller, T.; Baines, K.M. NH bond activation of ammonia and amines by ditetrelenes: Key insights into the stereochemistry of nucleophilic addition. *Dalton Trans.* **2021**, *50*, 17734–17750. [[CrossRef](#)] [[PubMed](#)]
94. Oláh, J.; Veszprémi, T. Mechanism of water addition to silatriafulvenes and silapentafulvenes. *Organometallics* **2008**, *27*, 2723–2729. [[CrossRef](#)]
95. Wang, Y.; Zeng, X. Comparative theoretical study on the addition reactions of MeOH to silabenzenes and germabenzenes. *Comput. Theor. Chem.* **2016**, *1078*, 88–95. [[CrossRef](#)]
96. Li, B.-Y.; Sheu, J.-H.; Su, M.-D. Mechanisms for the reaction of water, butadiene, and palladium complex with 1,2-dimetallacyclohexene ( $R_2M=MR_2$ , M = C, Si, Ge, Sn, Pb). A theoretical study. *Organometallics* **2011**, *30*, 4862–4872. [[CrossRef](#)]
97. Gaudel-Siri, A.; Pons, J.-M.; Piétri, N.; Tamburelli-Couturier, I.; Aycard, J.-P. Reaction of trimethylsilylketene with HCl: Mechanistic study. *Int. J. Quant. Chem.* **2006**, *106*, 719–726. [[CrossRef](#)]
98. Zhao, J.-X.; Xiao, B.; Ding, Y.-H. Theoretical prediction of the N–H and O–H bonds cleavage catalyzed by the single-walled silicon carbide nanotube. *J. Phys. Chem. C* **2009**, *113*, 16736–16740. [[CrossRef](#)]
99. Chen, Y.; Wang, F. Intermolecular interactions involving heavy alkenes H<sub>2</sub>Si=TH<sub>2</sub> (T = C, Si, Ge, Sn, Pb) with H<sub>2</sub>O and HCl: Tetrel bond and hydrogen bond. *ACS Omega* **2020**, *5*, 30210–30225. [[CrossRef](#)]
100. Owens, T.R.; Harrington, C.R.; Pace, T.C.S.; Leigh, W.J. Steric effects on silene reactivity. The effects of *ortho*-methyl substituents on the kinetics and mechanisms of the reactions of 1,1-diarylsilenes with nucleophiles. *Organometallics* **2003**, *22*, 5518–5525. [[CrossRef](#)]
101. Owens, T.R.; Grinyer, J.; Leigh, W.J. Direct detection of 1,1-diphenyl-2-neopentylsilene and the effects of solvent polarity on its reactivity with nucleophiles. *Organometallics* **2005**, *24*, 2307–2318. [[CrossRef](#)]
102. Iwamoto, T.; Abe, T.; Ishida, S.; Kabuto, C.; Kira, M. Reactions of trisilaallene and 2-germadisilaallene with various reagents. *J. Organomet. Chem.* **2007**, *692*, 263–270. [[CrossRef](#)]
103. Wang, X.H.; Zheng, C.C.; Ning, J.Q. Influence of curvature strain and van der Waals force on the interlayer vibration mode of WS<sub>2</sub> nanotubes: A confocal micro-Raman spectroscopic study. *Sci. Rep.* **2016**, *6*, 33091. [[CrossRef](#)]
104. Baxter, J.B.; Guglietta, G.W. Terahertz spectroscopy. *Anal. Chem.* **2011**, *83*, 4342–4368. [[CrossRef](#)] [[PubMed](#)]
105. Ueno, Y.; Ajito, K. Analytical terahertz spectroscopy. *Anal. Sci.* **2008**, *24*, 185–192. [[CrossRef](#)] [[PubMed](#)]
106. Plusquellic, D.F.; Siegrist, K.; Heilweil, E.J.; Esenturk, O. Applications of terahertz spectroscopy in biosystems. *ChemPhysChem* **2007**, *8*, 2412–2431. [[CrossRef](#)]
107. Kaplan, I.G. *Intermolecular Interactions: Physical Picture, Computational Methods and Model Potentials*; John Wiley & Sons, Ltd.: Chichester, UK, 2006. [[CrossRef](#)]
108. Casimir, H.B.G.; Polder, D. The influence of retardation on the London-van der Waals forces. *Phys. Rev.* **1948**, *73*, 360–372. [[CrossRef](#)]
109. Buhmann, S.Y. *Dispersion Forces I: Macroscopic Quantum Electrodynamics and Ground-State Casimir, Casimir–Polder and van der Waals Forces*, 1st ed.; Springer: Berlin/Heidelberg, Germany, 2012. [[CrossRef](#)]
110. Dalvit, D.; Milonni, P.; Roberts, D.; da Rosa, F. *Casimir Physics*, 1st ed.; Springer: Berlin/Heidelberg, Germany, 2011. [[CrossRef](#)]

111. Simpson, W.M.R.; Leonhardt, U. *Forces of the Quantum Vacuum: An Introduction to Casimir Physics*; World Scientific: Singapore, 2015. [[CrossRef](#)]
112. Takahashi, M.; Matsui, H.; Ikemoto, Y.; Suzuki, M.; Morimoto, N. Assessment of the VDW interaction converting DMAPS from the thermal-motion form to the hydrogen-bonded form. *Sci. Rep.* **2019**, *9*, 13104. [[CrossRef](#)]
113. Takahashi, M.; Chen, S.; Matsui, H.; Morimoto, N.; Ikemoto, Y. Van der Waals interactions regulating the hydration of 2-methacryloyloxyethyl phosphorylcholine, the constructing monomer of biocompatible polymers. *Sci. Rep.* **2022**, *12*, 20393. [[CrossRef](#)]
114. Takahashi, M.; Veszprémi, T.; Kira, M. Importance of frontier orbital interactions in addition reaction of water to disilene. *Int. J. Quant. Chem.* **2001**, *84*, 192–197. [[CrossRef](#)]
115. Ortiz, J.V. Electron binding energies of anionic alkali metal atoms from partial fourth order electron propagator theory calculations. *J. Chem. Phys.* **1988**, *89*, 6348–6352. [[CrossRef](#)]
116. Cederbaum, L.S. One-body Green's function for atoms and molecules: Theory and application. *J. Phys. B Atom. Mol. Phys.* **1975**, *8*, 290–303. [[CrossRef](#)]
117. von Niessen, W.; Schirmer, J.; Cederbaum, L.S. Computational methods for the one-particle Green's function. *Comput. Phys. Rep.* **1984**, *1*, 57–125. [[CrossRef](#)]
118. Zakrzewski, V.G.; von Niessen, W. Vectorizable algorithm for Green function and many-body perturbation methods. *J. Comput. Chem.* **1993**, *14*, 13–18. [[CrossRef](#)]
119. Nagase, S.; Kudo, T.; Ito, K. Structures, stability, and reactivity of doubly bonded compounds containing silicon or germanium. In *Applied Quantum Chemistry*, 1st ed.; Smith, V.H., Scheafer, H.F., Jr., Morokuma, K., Eds.; Springer: Dordrecht, The Netherlands, 1986; pp. 249–267. [[CrossRef](#)]
120. Becke, A.D. Density-functional thermochemistry. III. The role of exact exchange. *J. Chem. Phys.* **1993**, *98*, 5648–5652. [[CrossRef](#)]
121. Tsuneda, T.; Song, J.-W.; Suzuki, S.; Hirao, K. On Koopmans' theorem in density functional theory. *J. Chem. Phys.* **2010**, *133*, 174101. [[CrossRef](#)]
122. Yu, J.; Su, N.Q.; Yang, W. Describing chemical reactivity with frontier molecular orbitals. *JACS Au* **2022**, *2*, 1383–1394. [[CrossRef](#)]
123. Zhang, J.-X.; Sheong, F.K.; Lin, Z. Unravelling chemical interactions with principal interacting orbital analysis. *Chem. Eur. J.* **2018**, *24*, 9639–9650. [[CrossRef](#)] [[PubMed](#)]
124. Glendening, E.D.; Weinhold, F. Resonance natural bond orbitals: Efficient semilocalized orbitals for computing and visualizing reactive chemical processes. *J. Chem. Theory Comput.* **2019**, *15*, 916–921. [[CrossRef](#)]
125. Mosey, N.J.; Baines, K.M.; Woo, T.K. Mechanism of the addition of nonenolizable aldehydes and ketones to (di)metallenes ( $R_2X=YR_2$ ,  $X = Si, Ge$   $Y = C, Si, Ge$ ): A density functional and multiconfigurational perturbation theory study. *J. Am. Chem. Soc.* **2002**, *124*, 13306–13321. [[CrossRef](#)]
126. Yamabe, S.; Mizukami, N.; Tsuchida, N.; Yamazaki, S. A new mechanism for the addition of alcohols to disilenes revealed by DFT and ONIOM calculations. *J. Organomet. Chem.* **2008**, *693*, 1335–1345. [[CrossRef](#)]
127. Xu, Y.-J.; Zhang, Y.-F.; Li, J.-Q. Theoretical study of the hydroboration reaction of disilenes with borane. *Chem. Phys. Lett.* **2006**, *421*, 36–41. [[CrossRef](#)]
128. Li, B.-Y.; Su, M.-D. Theoretical investigation of the mechanisms for the reaction of fused tricyclic dimetallenes containing highly strained E=E ( $E = C, Si, Ge, Sn, \text{ and } Pb$ ) double bonds. *J. Phys. Chem. A* **2012**, *116*, 4222–4232. [[CrossRef](#)]
129. Liu, Y.; Yang, Y.; Zhu, R.; Liu, C.; Zhang, D. The dual role of gold(I) complexes in photosensitizer-free visible-light-mediated gold-catalyzed 1,2-difunctionalization of alkynes: A DFT study. *Chem. Eur. J.* **2018**, *24*, 14119–14126. [[CrossRef](#)] [[PubMed](#)]
130. Tashkandi, N.Y.; Bourque, J.L.; Baines, K.M. Reactivity of sulfonyl-containing compounds with ditetrelenes. *Dalton Trans.* **2017**, *46*, 15451–15457. [[CrossRef](#)] [[PubMed](#)]
131. Maity, B.; Koley, D. Computational investigation on the role of disilene substituents toward  $N_2O$  activation. *J. Phys. Chem. A* **2017**, *121*, 401–417. [[CrossRef](#)] [[PubMed](#)]
132. Maity, B.; Koley, D. Mechanistic investigation of the reactivity of disilene with nitrous oxide: A DFT study. *J. Mol. Graph. Model.* **2014**, *51*, 50–63. [[CrossRef](#)]
133. Li, B.-Y.; Su, M.-D. Theoretical investigations of the reactions of phosphino disilenes and their derivatives with an E=E ( $E = C, Si, Ge, Sn, \text{ and } Pb$ ) double bond. *J. Phys. Chem. A* **2012**, *116*, 9412–9420. [[CrossRef](#)]
134. Bitzer, T.; Richardson, N.V.; Schiffrin, D.J. The adsorption of alcohols on hydroxylated Si(100)-2 × 1. *Surf. Sci.* **1997**, *382*, L686–L689. [[CrossRef](#)]
135. Casaletto, M.P.; Zanoni, R.; Carbone, M.; Piancastelli, M.N.; Aballe, L.; Weiss, K.; Horn, K. High-resolution photoemission study of ethanol on Si(100)2 × 1. *Surf. Sci.* **2000**, *447*, 237–244. [[CrossRef](#)]
136. Lopez, A.; Bitzer, T.; Heller, T.; Richardson, N.V. Adsorption of water on alkoxy modified Si(100), Si(113) and Si (115) surfaces. *Surf. Sci.* **2001**, *473*, 108–116. [[CrossRef](#)]
137. Ehrley, W.; Butz, R.; Mantl, S. External infrared reflection absorption spectroscopy of methanol on an epitaxially grown Si(100)2 × 1 surface. *Surf. Sci.* **1991**, *248*, 193–200. [[CrossRef](#)]

138. Casaletto, M.P.; Zannoni, R.; Carbone, M.; Piancastelli, M.N.; Aballe, L.; Weiss, K.; Horn, K. Methanol adsorption on Si(100) $2 \times 1$  investigated by high-resolution photoemission. *Surf. Sci.* **2002**, *505*, 251–259. [[CrossRef](#)]
139. Zhang, L.; Carman, A.J.; Casey, S.M. Adsorption and thermal decomposition chemistry of 1-propanol and other primary alcohols on the Si(100) surface. *J. Phys. Chem. B* **2003**, *107*, 8424–8432. [[CrossRef](#)]
140. Buriak, J.M. Organometallic chemistry on silicon and germanium surfaces. *Chem. Rev.* **2002**, *102*, 1271–1308. [[CrossRef](#)] [[PubMed](#)]
141. Mulcahy, C.P.A.; Carman, A.J.; Casey, S.M. The adsorption and thermal decomposition of dimethylamine on Si(100). *Surf. Sci.* **2000**, *459*, 1–13. [[CrossRef](#)]
142. Mui, C.; Wang, G.T.; Bent, S.F.; Musgrave, C.B. Reactions of methylamines at the Si(100)- $2 \times 1$  surface. *J. Chem. Phys.* **2001**, *114*, 10170–10180. [[CrossRef](#)]
143. Cao, X.; Hamers, R.J. Silicon surfaces as electron acceptors: Dative bonding of amines with Si(001) and Si(111) surfaces. *J. Am. Chem. Soc.* **2001**, *123*, 10988–10996. [[CrossRef](#)]
144. Mui, C.; Han, J.H.; Wang, G.T.; Musgrave, C.B.; Bent, S.F. Proton transfer reactions on semiconductor surfaces. *J. Am. Chem. Soc.* **2002**, *124*, 4027–4038. [[CrossRef](#)]
145. Cao, X.; Hamers, R.J. Interactions of alkylamines with the silicon (001) surface. *J. Vac. Sci. Technol. B* **2002**, *20*, 1614–1619. [[CrossRef](#)]
146. Carman, A.J.; Zhang, L.; Liswood, J.L.; Casey, S.M. Methylamine adsorption on and desorption from Si(100). *J. Phys. Chem. B* **2003**, *107*, 5491–5502. [[CrossRef](#)]
147. Henry, A.T.; Bourque, J.L.; Vacirca, I.; Scheschkewitz, D.; Baines, K.M. The addition of a cyclopropyl alkyne to an asymmetrically-substituted disilene: A mechanistic study. *Organometallics* **2019**, *38*, 1622–1626. [[CrossRef](#)]
148. Leigh, W.J.; Owens, T.R.; Bendikov, M.; Zade, S.S.; Apeloig, Y. A combined experimental and theoretical study of the kinetics and mechanism of the addition of alcohols to electronically stabilized silenes: A new mechanism for the addition of alcohols to the Si=C bond. *J. Am. Chem. Soc.* **2006**, *128*, 10772–10783. [[CrossRef](#)] [[PubMed](#)]
149. Wiberg, N.; Niedermayer, W.; Polborn, K.; Mayer, P. Reactivity of the isolable disilene R\*PhSi=SiPhR\* (R\* = Si*t*Bu<sub>3</sub>). *Chem. Eur. J.* **2002**, *8*, 2730–2739. [[CrossRef](#)] [[PubMed](#)]
150. Kira, M.; Iwamoto, T. Progress in the chemistry of stable disilenes. *Adv. Organomet. Chem.* **2006**, *54*, 73–148. [[CrossRef](#)]
151. Kizhuvudath, A.; Mallikasseri, J.J.; Mathew, J. Electronic effects of substituents on the reactivity of silenes: A computational analysis. *Struct. Chem.* **2024**, *35*, 119–133. [[CrossRef](#)]
152. Huck, L.A.; Leigh, W.J. Substituent effects on the reactions of diarylgermylenes and tetraaryldigermenes with acetic acid and other Lewis bases in hydrocarbon solution. *Organometallics* **2007**, *26*, 1339–1348. [[CrossRef](#)]
153. Leigh, W.J.; Boukherroub, R.; Kerst, C. Substituent effects on the reactivity of the silicon–carbon double bond. Resonance, inductive, and steric effects of substituents at silicon on the reactivity of simple 1-methylsilenes. *J. Am. Chem. Soc.* **1998**, *120*, 9504–9512. [[CrossRef](#)]
154. Leigh, W.J.; Kerst, C.; Boukherroub, R.; Morkin, T.L.; Jenkins, S.I.; Sung, K.; Tidwell, T.T. Substituent effects on the reactivity of the silicon–carbon double bond. Substituted 1,1-dimethylsilenes from far-UV laser flash photolysis of  $\alpha$ -silylketenes and (trimethylsilyl)diazomethane. *J. Am. Chem. Soc.* **1999**, *121*, 4744–4753. [[CrossRef](#)]
155. Guliasvili, T.; Tibbelin, J.; Ryu, J.; Ottosson, H. Unsuccessful attempts to add alcohols to transient 2-amino-2-siloxy-silenes—Leading to a new benign route for base-free alcohol protection. *Dalton Trans.* **2010**, *39*, 9379–9385. [[CrossRef](#)]
156. Gridnev, I.D. Sigmatropic and haptotropic rearrangements in organometallic chemistry. *Coordin. Chem. Rev.* **2008**, *252*, 1798–1818. [[CrossRef](#)]
157. Woodward, R.B.; Hoffman, R. *The Conservation of Orbital Symmetry*, 2nd ed.; Academic Press: New York, NY, USA, 1970.
158. Kwart, H.; Slutsky, J. Unimolecular thermal rearrangement of allylsilanes. A sigmatropic 1,3 migration of silicon. *J. Am. Chem. Soc.* **1972**, *94*, 2515–2516. [[CrossRef](#)]
159. Slutsky, J.; Kwart, H. The kinetics, stereochemistry, and mechanisms of the silylallylic and silylpropynylic rearrangements. *J. Am. Chem. Soc.* **1973**, *95*, 8678–8685. [[CrossRef](#)]
160. Takahashi, M.; Kira, M. A theoretical study of stereochemistry of 1,3-migration in allylsilane and related allylmetallic compounds. *J. Am. Chem. Soc.* **1997**, *119*, 1948–1953. [[CrossRef](#)]
161. Yamabe, T.; Nakamura, K.; Shiota, Y.; Yoshizawa, K.; Kawauchi, S.; Ishikawa, M. Novel aspects of the [1,3] sigmatropic silyl shift in allylsilane. *J. Am. Chem. Soc.* **1997**, *119*, 807–815. [[CrossRef](#)]
162. Zhang, L.C.; Kabuto, C.; Kira, M. Retention stereochemistry of thermal 1,3-silyl migration in allylsilanes. *J. Am. Chem. Soc.* **1999**, *121*, 2925–2926. [[CrossRef](#)]
163. Rynin, S.S.; Faustov, V.I.; Boganov, S.E.; Egorov, M.P.; Nefedov, O.M. GeCl<sub>2</sub> cycloaddition reactions to unsaturated organic compounds taking ethylene, buta-1,3-diene, and hexa-1,3,5-triene as examples: A quantum chemical study. *Russ. Chem. Bull. Int. Ed.* **2010**, *59*, 1099–1109. [[CrossRef](#)]
164. Rynin, S.S.; Faustov, V.I.; Boganov, S.E.; Egorov, M.P.; Nefedov, O.M. Computational study of reaction pathways in the course of interaction of deactivated silylenes with buta-1,3-diene. *J. Organomet. Chem.* **2010**, *695*, 2345–2353. [[CrossRef](#)]

165. Rynin, S.S.; Kulikov, P.V.; Faustov, V.I.; Boganov, S.E.; Egorov, M.P.; Nefedov, O.M. Computational study of 2-vinylsilirane to silacyclopent-3-ene rearrangement. *J. Mol. Struct. THEOCHEM* **2010**, *942*, 60–65. [CrossRef]
166. Lim, C.; Lee, H.; Kwak, Y.-W.; Choi, C.H. A theoretical study of thermal [1,3]-sigmatropic rearrangements of 3-trimethylsilyl-1-pyrazoline: Concerted vs. stepwise mechanisms. *J. Comput. Chem.* **2006**, *27*, 228–237. [CrossRef]
167. Shi, J.; Li, L.; Shan, C.; Wang, J.; Chen, Z.; Gu, R.; He, J.; Tan, M.; Lan, Y.; Li, Y. Aryne 1,2,3,5-tetrasubstitution enabled by 3-silylaryne and allyl sulfoxide via an aromatic 1,3-silyl migration. *J. Am. Chem. Soc.* **2021**, *143*, 2178–2184. [CrossRef]
168. Makita, K.; Koketsu, J.; Ando, F.; Ninomiya, Y.; Koga, N. Theoretical investigation of Stevens rearrangement of P and As ylides. Migration of H, CH<sub>3</sub>, CH=CH<sub>2</sub>, SiH<sub>3</sub>, and GeH<sub>3</sub> groups on P and As atoms. *J. Am. Chem. Soc.* **1998**, *120*, 5764–5770. [CrossRef]
169. Brook, A.G.; MacRae, D.M.; Limburg, W.W. Stereochemistry of the formation and thermal rearrangement of β-ketosilanes. *J. Am. Chem. Soc.* **1967**, *89*, 5493–5495. [CrossRef]
170. Takahashi, M.; Kira, M. A theoretical study of mechanisms of 1,3-silyl migration in formylmethylsilane and related migrations. Comparison with allylsilane. *J. Am. Chem. Soc.* **1999**, *121*, 8597–8603. [CrossRef]
171. Berson, J.A.; Salem, L. Subjacent orbital control. An electronic factor favoring concertedness in Woodward–Hoffmann “forbidden” reactions. *J. Am. Chem. Soc.* **1972**, *94*, 8917–8918. [CrossRef]
172. Berson, J.A. Orbital-symmetry-forbidden reactions. *Acc. Chem. Res.* **1972**, *5*, 406–414. [CrossRef]
173. Li, H.; Liu, L.; Wang, Z.; Zhao, F.; Zhang, S.; Zhang, W.-X.; Xi, Z. Iterative dianion relay along the ring: Formation of gem-bis(trimethylsilyl) cyclopentenones from 2,5-bis(trimethylsilyl) oxy-cyclopentadienyl dianions and acid chlorides. *Chem. Eur. J.* **2011**, *17*, 7399–7403. [CrossRef]
174. Oblin, M.; Fotiadu, F.; Rajzmann, M.; Pons, J.-M. Formation of silylketenes via a 1,3-silyl shift. A theoretical study. *J. Chem. Soc. Perkin Trans.* **1997**, *2*, 1621–1623. [CrossRef]
175. Yoshizawa, K.; Kondo, Y.; Kang, S.-Y.; Naka, A.; Ishikawa, M. Role of diagonal silicon–carbon interaction in the [2 + 2] cycloaddition of silene and acetylene. *Organometallics* **2002**, *21*, 3271–3277. [CrossRef]
176. Muhammed, S.; Parameswaran, P. Mechanistic insights into the [3+1] cycloadditions of Me<sub>3</sub>SiN<sub>3</sub> on bis-silylene and the formation of pseudo-silaazatriene. *Eur. J. Inorg. Chem.* **2024**, *27*, e202400031. [CrossRef]
177. Bevern, D.; Pröhl, F.E.; Görls, H.; Kriek, S.; Westerhausen, M. Versatile access to very short P=P double bonds in mixed-valent 1λ<sup>5</sup>-diphosphenes via 1,3-silyl migration. *Organometallics* **2021**, *40*, 1744–1750. [CrossRef]
178. Shen, H.; Xiao, X.; Hoye, T.R. Benzyne cascade reactions via benzoxetenonium ions and their rearrangements to *o*-quinone methides. *Org. Lett.* **2019**, *21*, 1672–1675. [CrossRef]
179. Tang, J.; Ming, L.; Zhao, X. Sulfur heterocyclization and 1,3-migration of silicon in reaction of 1,3-diynes with sodium triisopropylsilylanethiolate: One-pot synthesis of 2,5-disubstituted 3-(triisopropylsilyl)thiophenes. *Synthesis* **2013**, *45*, 1713–1718. [CrossRef]
180. Austin, W.F.; Zhang, Y.; Danheiser, R.L. A benzannulation strategy for the synthesis of phenols and heteroaromatic compounds based on the reaction of (trialkylsilyl)vinylketenes with lithium ynolates. *Tetrahedron* **2008**, *64*, 915–925. [CrossRef] [PubMed]
181. Nakamura, I.; Sato, T.; Terada, M.; Yamamoto, Y. Gold-catalyzed cyclization of (*ortho*-alkynylphenylthio)silanes: Intramolecular capture of the vinyl-Au intermediate by the silicon electrophile. *Org. Lett.* **2007**, *9*, 4081–4083. [CrossRef] [PubMed]
182. Chiara, J.L.; García, Á.; Sesiñlo, E.; Vacas, T. 1-Silyl-2,6-diketones: Versatile intermediates for the divergent synthesis of five- and six-membered carbocycles under radical and anionic conditions. *Org. Lett.* **2006**, *8*, 3935–3938. [CrossRef]
183. Campomanes, P.; Menéndez, M.I.; Sordo, T.L. Mechanism of cycloaddition reactions between ketene and n-silyl-, n-germyl-, and n-stannylimines: A theoretical investigation. *J. Phys. Chem. A* **2005**, *109*, 11022–11026. [CrossRef]
184. Austin, W.F.; Zhang, Y.; Danheiser, R.L. Reactions of (trialkylsilyl)vinylketenes with lithium ynolates: A new benzannulation strategy. *Org. Lett.* **2005**, *7*, 3905–3908. [CrossRef]
185. Jia, Z.; Feng, S.; Song, E.; Sun, W.; Cong, L. Theoretical study on the mechanism for the thermal rearrangement reactions of 2-silylethyl acetate H<sub>3</sub>SiCH<sub>2</sub>CH<sub>2</sub>OCOCH<sub>3</sub>. *Int. J. Quant. Chem.* **2009**, *109*, 342–348. [CrossRef]
186. Shiina, I.; Nagasue, H. [1,3] Sigmatropic rearrangement of ketene silyl acetals derived from benzyl α-substituted propanoates. *Tetrahedron Lett.* **2002**, *43*, 5837–5840. [CrossRef]
187. Hou, S.; Li, X.; Xu, J. N [1,3]-sigmatropic shift in the benzidine rearrangement: Experimental and theoretical investigation. *Org. Biomol. Chem.* **2014**, *12*, 4952–4963. [CrossRef]
188. Bernardi, F.; Olivucci, M.; Robb, M.A.; Tonachini, G. Can a photochemical reaction be concerted? A theoretical study of the photochemical sigmatropic rearrangement of but-1-ene. *J. Am. Chem. Soc.* **1992**, *114*, 5805–5812. [CrossRef]
189. Rossi, I.; Bernardi, F.; Olivucci, M.; Robb, M.A. Falling down the singlet manifold. A CAS-SCF mechanistic study of the far-UV photochemistry of hexa-1,5-dienes. *J. Phys. Chem.* **1995**, *99*, 6757–6759. [CrossRef]
190. Freund, L.; Klessinger, M. Photochemical reaction pathways of ethylene. *Int. J. Quant. Chem.* **1998**, *70*, 1023–1028. [CrossRef]
191. Wilsey, S.; Houk, K.N.; Zewail, A.H. Ground- and excited-state reactions of norbornene and isomers: A CASSCF study and comparison with femtosecond experiments. *J. Am. Chem. Soc.* **1999**, *121*, 5772–5786. [CrossRef]

192. Steuhl, H.-M.; Bornemann, C.; Klessinger, M. The mechanism of the photochemical hydrogen migration in 1,3,5-cycloheptatriene: A theoretical study. *Chem. Eur. J.* **1999**, *5*, 2404–2412. [[CrossRef](#)]
193. Bornemann, C.; Klessinger, M. Excited-state energy and geometry changes during the [1,7]H-shift reaction of cycloheptatriene. *Org. Lett.* **1999**, *1*, 1889–1891. [[CrossRef](#)]
194. Wilsey, S.; Houk, K.N. H/allyl and alkyl/allyl conical intersections: Ubiquitous control elements in photochemical sigmatropic shifts. *J. Am. Chem. Soc.* **2000**, *122*, 2651–2652. [[CrossRef](#)]
195. Bernardi, F.; Olivucci, M.; Robb, M.A.; Vreven, T.; Soto, J. An ab initio study of the photochemical decomposition of 3,3-dimethyldiazirine. *J. Org. Chem.* **2000**, *65*, 7847–7857. [[CrossRef](#)]
196. Fuss, W.; Schmid, W.E.; Trushin, S.A. Ultrafast dynamics of cyclohexene and cyclohexene-*d*<sub>10</sub> excited at 200 nm. *J. Am. Chem. Soc.* **2001**, *123*, 7101–7108. [[CrossRef](#)]
197. Wilsey, S.; Houk, K.N. “H/vinyl” and “alkyl/vinyl” conical intersections leading to carbene formation from the excited states of cyclohexene and norbornene. *J. Am. Chem. Soc.* **2002**, *124*, 11182–11190. [[CrossRef](#)]
198. Garavelli, M.; Bernardi, F.; Cembran, A.; Castaño, O.; Frutos, L.M.; Merchán, M.; Olivucci, M. Cyclooctatetraene computational photo- and thermal chemistry: A reactivity model for conjugated hydrocarbons. *J. Am. Chem. Soc.* **2002**, *124*, 13770–13789. [[CrossRef](#)]
199. Takahashi, M.; Sakamoto, K. Ab initio study of the photochemistry of *c*-C<sub>2</sub>H<sub>2</sub>Si. *J. Phys. Chem. A* **2004**, *108*, 7301–7305. [[CrossRef](#)]
200. Su, M.-D. A mechanistic study of the addition of alcohol to a five-membered ring silene via a photochemical reaction. *Phys. Chem. Chem. Phys.* **2016**, *18*, 8228–8234. [[CrossRef](#)] [[PubMed](#)]
201. Su, M.-D. A model study on the photochemical isomerization of cyclic silenes. *Phys. Chem. Chem. Phys.* **2015**, *17*, 5039–5042. [[CrossRef](#)] [[PubMed](#)]
202. Varras, P.C.; Zarkadis, A.K. Ground- and triplet excited-state properties correlation: A computational CASSCF/CASPT2 approach based on the photodissociation of allylsilanes. *J. Phys. Chem. A* **2012**, *116*, 1425–1434. [[CrossRef](#)]
203. Cordova, F.; Doriol, L.J.; Ipatov, A.; Casida, M.E.; Filippi, C.; Vela, A. Troubleshooting time-dependent density-functional theory for photochemical applications: Oxirane. *J. Chem. Phys.* **2007**, *127*, 164111. [[CrossRef](#)]
204. Drzewiecka-Matuszek, A.; Rutkowska-Zbik, D. Application of TD-DFT theory to studying porphyrinoid-based photosensitizers for photodynamic therapy: A review. *Molecules* **2021**, *26*, 7176. [[CrossRef](#)]
205. Yao, G.; Pradhan, E.; Yang, Z.; Zeng, T. Ligand impacts on band edge energies and excited state splittings of silicane. *Phys. Chem. Chem. Phys.* **2025**, *27*, 4845–4857. [[CrossRef](#)]
206. Yang, S.; Lan, Y.; Li, G.; Peng, B.; Guo, H. Study of photoinduced nonthermal melting of 4H-SiC under femtosecond pulse laser irradiation based on time-dependent density functional theory simulations. *J. Appl. Phys.* **2024**, *136*, 245701. [[CrossRef](#)]
207. Douglas-Gallardo, O.A.; Sánchez, C.G.; Vöhringer-Martinez, E. Communication: Photoinduced carbon dioxide binding with surface-functionalized silicon quantum dots. *J. Chem. Phys.* **2018**, *148*, 141102. [[CrossRef](#)]
208. Yang, J.; Fang, H.; Gao, Y. Microscopic mechanism for light-induced degradation of silicon solar cell in water vapor environment. *Nano Energy* **2016**, *30*, 614–620. [[CrossRef](#)]
209. Zwijnenburg, M.A.; Sokol, A.A.; Sousa, C.; Bromley, S.T. The effect of local environment on photoluminescence: A time-dependent density functional theory study of silanone groups on the surface of silica nanostructures. *J. Chem. Phys.* **2009**, *131*, 034705. [[CrossRef](#)] [[PubMed](#)]
210. Thaddeus, P.; Vrtilik, J.M.; Gottlieb, C.A. Laboratory and astronomical identification of cyclopropenylidene, C<sub>3</sub>H<sub>2</sub>. *Astrophys. J.* **1985**, *299*, L63–L66. [[CrossRef](#)]
211. Adams, N.G.; Smith, D. On the synthesis of *c*-C<sub>3</sub>H<sub>2</sub> in interstellar clouds. *Astrophys. J.* **1987**, *317*, L25–L27. [[CrossRef](#)]
212. Cernicharo, J.; Gottlieb, C.A.; Guélin, M.; Killian, T.C.; Paubert, G.; Thaddeus, P.; Vrtilik, J.M. Astronomical detection of H<sub>2</sub>CCC. *Astrophys. J.* **1991**, *368*, L39–L41. [[CrossRef](#)]
213. Gottlieb, C.A.; Killian, T.C.; Thaddeus, P.; Botschwina, P.; Flügge, J.; Oswald, M. Structure of propadienylidene, H<sub>2</sub>CCC. *J. Chem. Phys.* **1993**, *98*, 4478–4485. [[CrossRef](#)]
214. Srinivas, R.; Sülzle, D.; Weiske, T.; Schwarz, H. Generation and characterization of neutral and cationic 3-sila-cyclopropenylidene in the gas phase: Description of a new BEBE tandem mass spectrometer. *Int. J. Mass Spectrom. Ion Process.* **1991**, *107*, 369–376. [[CrossRef](#)]
215. Maier, G.; Reisenauer, H.P.; Schwab, W.; Čársky, P.; Hess, B.A., Jr.; Schaad, L.J. Vinylidenecarbene: A new C<sub>3</sub>H<sub>2</sub> species. *J. Am. Chem. Soc.* **1987**, *109*, 5183–5188. [[CrossRef](#)]
216. Maier, G.; Pacl, H.; Reisenauer, H.P.; Meudt, A.; Janoschek, R. Silacyclopropyne: Matrix spectroscopic identification and ab initio investigations. *J. Am. Chem. Soc.* **1995**, *117*, 12712–12720. [[CrossRef](#)]
217. Rettig, A.; Head-Gordon, M.; Doddipatla, S.; Yang, Z.; Kaiser, R.I. Crossed beam experiments and computational studies of pathways to the preparation of singlet ethynylsilylene (HCCSiH; X<sup>1</sup>A′): The silacarbene counterpart of triplet propargylene (HCCCH; X<sup>3</sup>B). *J. Phys. Chem. Lett.* **2021**, *12*, 10768–10776. [[CrossRef](#)]
218. Saxe, P.; Schaefer, H.F., III. Can cyclopropyne really be made? *J. Am. Chem. Soc.* **1980**, *102*, 3239–3240. [[CrossRef](#)]

219. Fitzgerald, G.; Schaefer, H.F., III. Structures, energetics and vibrational frequencies of cyclopropyne. *Isr. J. Chem.* **1983**, *23*, 93–96. [[CrossRef](#)]
220. Frenking, G.; Remington, R.B.; Schaefer, H.F., III. Structures and energies of singlet silacyclopropenylidene and 14 higher lying  $C_2SiH_2$  isomers. *J. Am. Chem. Soc.* **1986**, *108*, 2169–2173. [[CrossRef](#)] [[PubMed](#)]
221. Su, M.-D.; Amos, R.D.; Handy, N.C. A Theoretical study of the reaction of ground-state silicon with ethylene and acetylene. *J. Am. Chem. Soc.* **1990**, *112*, 1499–1504. [[CrossRef](#)]
222. Cooper, D.L. Ab initio predictions for silicon analogs of astrophysically interesting molecules:  $SiC_2H_2$ ,  $SiH_2CN$ ,  $SiH_2C_2$ , and  $CH_2CSi$ . *Astrophys. J.* **1990**, *354*, 229–231. [[CrossRef](#)]
223. Vacek, G.; Colegrove, B.T.; Schaefer, H.F., III. The infrared spectrum of silacyclopropenylidene. *J. Am. Chem. Soc.* **1991**, *113*, 3192–3193. [[CrossRef](#)]
224. Sherrill, C.D.; Brandow, C.G.; Allen, W.D.; Schaefer, H.F., III. Cyclopropyne and silacyclopropyne: A world of difference. *J. Am. Chem. Soc.* **1996**, *118*, 7158–7163. [[CrossRef](#)]
225. Wu, Q.; Simmonett, A.C.; Yamaguchi, Y.; Li, Q.; Schaefer, H.F., III. Silacyclopropenylidene and its most important  $SiC_2H_2$  isomers. *J. Phys. Chem. C* **2010**, *114*, 5447–5457. [[CrossRef](#)]
226. Hao, Q.; Sommonett, A.C.; Yamaguchi, Y.; Fang, D.-C.; Schaefer, H.F., III. From acetylene complexes to vinylidene structures: The  $GeC_2H_2$  System. *J. Comput. Chem.* **2011**, *32*, 15–22. [[CrossRef](#)]
227. Job, N.; Karton, A.; Thirumoorthy, K.; Cooksy, A.L.; Thimmakonda, V.S. Theoretical studies of  $SiC_4H_2$  isomers delineate three low-lying silylidenes are missing in the laboratory. *J. Phys. Chem. A* **2020**, *124*, 987–1002. [[CrossRef](#)]
228. Thirumoorthy, K.; Cooksy, A.L.; Thimmakonda, V.S.  $Si_2C_5H_2$  isomers—Search algorithms *versus* chemical intuition. *Phys. Chem. Chem. Phys.* **2020**, *22*, 5865–5872. [[CrossRef](#)]
229. Ishikawa, M.; Nakagawa, K.; Ishiguro, M.; Ohi, F.; Kumada, M. Photolysis of organopolysilanes. The reaction of photochemically generated methylphenylsilylene with olefins. *J. Organomet. Chem.* **1978**, *152*, 155–174. [[CrossRef](#)]
230. Kira, M.; Taki, T.; Sakurai, H. Photochemical 1,3-silyl migration in allylsilanes occurring with inversion of silyl configuration. *J. Org. Chem.* **1989**, *54*, 5647–5648. [[CrossRef](#)]
231. Ishikawa, M.; Fuchikami, T.; Sugaya, T.; Kumada, M. Photolysis of organopolysilanes. A novel addition reaction of aryl substituted disilanes to olefins. *J. Am. Chem. Soc.* **1975**, *97*, 5923–5924. [[CrossRef](#)]
232. Sakurai, H.; Kamiyama, Y.; Nakadaira, Y. New photochemical reactions of vinyldisilanes through silaethene or silacyclopropane intermediates. *J. Am. Chem. Soc.* **1976**, *98*, 7424–7425. [[CrossRef](#)]
233. Ishikawa, M.; Fuchikami, T.; Kumada, M. Photochemically generated silicon–carbon double-bonded intermediates. VII. A new route to silaethene derivatives from 1-alkenyl-disilanes. *J. Organomet. Chem.* **1978**, *149*, 37–48. [[CrossRef](#)]
234. Brook, A.G.; Harris, J.W.; Lennon, J.; Sheikh, M.E. Relatively stable silaethylenes. Photolysis of acylpolysilanes. *J. Am. Chem. Soc.* **1979**, *101*, 83–95. [[CrossRef](#)]
235. Baines, K.M.; Brook, A.G. Photolysis of acylpolysilanes containing  $\alpha$ -hydrogens. Formation of linear head-to-head silene dimers. *Organometallics* **1987**, *6*, 692–696. [[CrossRef](#)]
236. Wright, B.B. A novel photorearrangement of 1-silyl 1,2-diones: Generation of siloxyketenes. *J. Am. Chem. Soc.* **1988**, *110*, 4456–4457. [[CrossRef](#)]
237. Ishikawa, M.; Sakamoto, H. Silicon–carbon unsaturated compounds. XXXII. Photolysis of tolyl- and xylylpentamethyldisilanes. *J. Organomet. Chem.* **1991**, *414*, 1–10. [[CrossRef](#)]
238. Ishikawa, M.; Nishimura, Y.; Sakamoto, H. Silicon–carbon unsaturated compounds. 33. Regiochemistry in the photochemical formation of silenes from 1,2,2,2-tetramethyl-, 1,1,2,2-tetramethyl-, and 2-ethyl-1,2,2-trimethylphenylvinylidene. *Organometallics* **1991**, *10*, 2701–2706. [[CrossRef](#)]
239. Takaki, K.; Sakamoto, H.; Nishimura, Y.; Sugihara, Y.; Ishikawa, M. Silicon–carbon unsaturated compounds. 28. Regiochemistry in the photochemical formation of silenes from dihydropyran-yl-substituted phenyldisilanes. *Organometallics* **1991**, *10*, 888–893. [[CrossRef](#)]
240. Böske, J.; Niecke, E.; Krebs, B.; Läge, M.; Henkel, G. 1,2-Dihydro-1,3,2 $\lambda^5$ ,4 $\lambda^5$ -diazadiphosphet—Synthesis, structure and isomerization to the “inner salt” of 1,3,2,4 $\lambda^5$ -diazadiphosphetan-2-ium hydroxide. *Chem. Ber.* **1992**, *125*, 2631–2634. [[CrossRef](#)]
241. Kira, M.; Miyazawa, T.; Sugiyama, H.; Yamaguchi, M.; Sakurai, H.  $\sigma\pi^*$  Orthogonal intramolecular charge-transfer (OICT) excited states and photoreaction mechanism of trifluoromethyl-substituted phenyldisilanes. *J. Am. Chem. Soc.* **1993**, *115*, 3116–3124. [[CrossRef](#)]
242. Ohshita, J.; Niwa, H.; Ishikawa, M.; Yamabe, T.; Yoshii, T.; Nakamura, K. Silicon–carbon unsaturated compounds. 57. Photolysis of *meso*- and *racemic*-1,2-diethyl-1,2-dimethyldiphenyldisilane, direct evidence for a concerted 1,3-silyl shift to *ortho*-carbon in the phenyl ring. *J. Am. Chem. Soc.* **1996**, *118*, 6853–6859. [[CrossRef](#)]
243. Miyazawa, T.; Koshihara, S.; Liu, C.; Sakurai, H.; Kira, M. Mechanistic studies of photochemical silylene extrusion from 2,2-diphenylhexamethyltrisilane. *J. Am. Chem. Soc.* **1999**, *121*, 3651–3656. [[CrossRef](#)]

244. Zhang, Z.; Wu, S.; Zhou, Y.; Li, B.-L.; Xiao, S.; Zhao, X.; Yu, Z. Visible-light-induced [1,3]-brook rearrangements of  $\alpha$ -ketoacylsilanes and their subsequent trapping in a tandem annulation with 1,3,5-triazinanes and azomethine imines. *Org. Chem. Front.* **2024**, *11*, 3250–3256. [[CrossRef](#)]
245. Ye, J.-H.; Bellotti, P.; Paulisch, T.O.; Daniliuc, C.G.; Glorius, F. Visible-light-induced cycloaddition of  $\alpha$ -ketoacylsilanes with imines: Facile access to  $\beta$ -lactams. *Angew. Chem. Int. Ed.* **2021**, *60*, 13671–13676. [[CrossRef](#)]
246. Brook, A.G. Some molecular rearrangements of organosilicon compounds. *Acc. Chem. Res.* **1974**, *7*, 77–84. [[CrossRef](#)]
247. Takahashi, M. The mechanism of photochemical 1,3-silyl migration of allylsilane. *J. Phys. Chem. A* **2005**, *109*, 11902–11906. [[CrossRef](#)]
248. Hammer, N.; Christensen, M.L.; Chen, Y.; Naharro, D.; Liu, F.; Jørgensen, K.A.; Houk, K.N. An experimental stereoselective photochemical [1s,3s]-sigmatropic silyl shift and the existence of silyl/allyl conical intersections. *J. Am. Chem. Soc.* **2020**, *142*, 6030–6035. [[CrossRef](#)]

**Disclaimer/Publisher’s Note:** The statements, opinions and data contained in all publications are solely those of the individual author(s) and contributor(s) and not of MDPI and/or the editor(s). MDPI and/or the editor(s) disclaim responsibility for any injury to people or property resulting from any ideas, methods, instructions or products referred to in the content.